

# Spatio-Temporal Variation in Stable Isotope and Elemental Composition of Key-Species Reflect Environmental changes in the Baltic Sea

Camilla LIENART (✉ [camilla.lienart@su.se](mailto:camilla.lienart@su.se))

Stockholms Universitet <https://orcid.org/0000-0001-5945-9869>

Andrius GARBARAS

Center for Physical Sciences and Technology, Vilnius, Lithuania

Susanne QVARFORDT

Stockholm University: Stockholms Universitet

Jakob WALVE

Stockholm University: Stockholms Universitet

Agnes ML Karlson

Stockholm University: Stockholms Universitet

---

## Research Article

**Keywords:** isotope baseline, amino-acid,  $\delta^{15}\text{N}$ , bioindicator, long-term environmental research (LTER), marine monitoring, biogeochemical cycles

**Posted Date:** May 25th, 2021

**DOI:** <https://doi.org/10.21203/rs.3.rs-550723/v1>

**License:** © ⓘ This work is licensed under a Creative Commons Attribution 4.0 International License. [Read Full License](#)

---

**Version of Record:** A version of this preprint was published at Biogeochemistry on November 11th, 2021. See the published version at <https://doi.org/10.1007/s10533-021-00865-w>.

# Abstract

Carbon and nitrogen stable isotope ratios are increasingly used to study long-term change in food web structure and nutrient cycling. Whether isotope composition in primary producers and consumers (so-called isotope baselines) reflect environmental changes in a similar manner is largely unknown. We take advantage of long-term oceanographic monitoring data and archived biological samples for the well-studied Baltic Sea to retrospectively analyse elemental composition (C, N and P) and stable isotopes ( $\delta^{13}\text{C}$ ,  $\delta^{15}\text{N}$ ) in the filamentous ephemeral macroalgae *Cladophora* spp. and in blue mussel *Mytilus edulis trossulus* from three contrasting regions (coastal Bothnian Sea and Baltic proper, open sea central Baltic) with the aim to statistically link the observed spatial and interannual (8–24 years' time-series) variability in elemental and isotope baselines with environmental changes. We find clear differences in isotope baselines between the two major Baltic Sea basins. However, the temporal development in *Mytilus*  $\delta^{13}\text{C}$  was remarkably similar among regions and, at the open sea station, mussels and algae  $\delta^{13}\text{C}$  also correlated over time, likely reflecting a global Baltic Sea or Northern Hemisphere pattern. In contrast,  $\delta^{15}\text{N}$  of both taxa responded to regional and local drivers (water nutrient concentrations).  $\delta^{15}\text{N}$  in source amino acids allowed detection of diazotrophic N signal in *Mytilus*, which was masked in bulk  $\delta^{15}\text{N}$ . Finally, *Cladophora* N:P reflected regional nutrient levels in the water while P %, which differed for both taxa, was linked to food quality for *Mytilus*. This study highlights the potential of a multi-taxa and multi-stable isotope approach to understand nutrient dynamics and monitor long-term environmental changes.

## 1. Introduction

Coastal seas are highly involved in fundamental biogeochemical processes controlling nutrient and organic matter cycling (Middelburg and Herman 2007; Bouwman et al. 2013; Carstensen et al. 2020). They receive nutrients and organic matter from both marine (e.g. primary production) and terrestrial (e.g. riverine inputs of terrestrial material, anthropogenic outfalls) origins and act as a filter between both realms (Asmala et al. 2017). In addition to climate change, human activities influence nutrient cycling through eutrophication, resulting in changes in both absolute values and ratios between nitrogen (N) and phosphorus (P). Major changes in nutrient supply are likely to affect primary producers' requirements with regard to elemental building blocks, and have repercussions on processes regulating consumers elemental homeostasis (ecological stoichiometry sensu Sterner and Elser 2002) with consequences for food web functioning and biogeochemical cycling.

Archived biological samples from environmental monitoring programs can be retrospectively analysed for elemental composition (C, N, P) and stable isotope ratios of carbon and nitrogen ( $\delta^{13}\text{C}$ ,  $\delta^{15}\text{N}$ ) to study nutrient cycling and reconstruct food webs in relation to a changing environment. Carbon isotopes provide information about ultimate carbon sources for primary production (Fry and Sherr 1984), while nitrogen isotopes can be used to trace specific nitrogen sources, such as anthropogenic (e.g. Connolly et al. 2013) or diazotrophic sources (Rolff 2000; Karlson et al. 2015), or to quantify trophic position in consumers (Vander Zanden and Rasmussen 1999). Organisms at the base of the food web such as filter-feeding bivalves or grazing snails, with low motility and long-life span, can be used as proxies for isotope baselines (i.e. the ultimate C and N sources) since they integrate intra-annual variability of nutrients (Vander Zanden and Rasmussen 1999; Post 2002). Perennial macrophytes typically reflect nutrient sources during the growth period (e.g. Savage and Elmgren 2004), hence the relatively fast turnover rates of macrophyte tissue may allow for the detection of subtle variations in N sources compared consumers such as bivalves, which provide an integrated measure of N signal over longer time spans, several months or even year(s) (Post 2002). Whether primary producers and primary consumers reflect large-scale and decadal changes in nutrient conditions in a similar manner is largely unknown.

In the Baltic Sea, the suspension-feeding blue mussel *Mytilus edulis trossulus* species complex (Kijewski et al. 2006; Stuckas et al. 2009; hereafter referred to as *Mytilus* or blue mussel) and the ephemeral filamentous green algae from the genus *Cladophora* are highly abundant. *Mytilus* occur in densities of up to  $\sim 100\,000$  individuals  $\text{m}^{-2}$  (Westerbom et al. 2008) and constitute, through their efficient suspension-feeding, an important link between the pelagic and benthic ecosystem, promoting nutrient cycling (Kautsky and Wallentinus 1980; Kautsky and Evans 1987; Attard et al. 2020). *Cladophora* is widely

distributed in the Baltic Sea (Zulkifly et al. 2013), and mainly occurs from the surface down to 1 or 2 m depths. It is perennial, but overwinters as a small tuft attached to shallow rocky substrates. During summer it reaches its full growth and benefits from nutrient enrichment (Thybo-christesen et al. 1993). Isotope composition in bivalves, including *Mytilus*, is commonly used to study pelagic organic matter origin (Magni et al. 2013) and its variability over time and space (Briant et al. 2018; Corman et al. 2018). Bivalves are considered suitable baselines for food web studies (e.g. Abrantes and Sheaves 2009; Willis et al. 2017) and in contaminant monitoring (Karlson and Faxneld 2021). *Cladophora* is mainly used as a proxy of nutrient levels in coastal waters, in the Baltic as well as elsewhere (Mäkinen and Aulio 1986; Planas et al. 1996).

The pronounced latitudinal gradients of temperature, salinity and nutrients combined with the historical excessive anthropogenic nutrient inputs in the Baltic Sea provide an ideal study system to link environmental and nutrient conditions with those measured in archived mussels and algae. Riverine inputs of organic carbon and nutrients have increased in the recent time period, especially in the Bothnian Sea (Wikner and Andersson 2012; Asmala et al. 2019), and this 'brownification' increase is expected to continue (Andersson et al. 2015a). In the Bothnian Sea, the N:P ratio of the dissolved inorganic pool is similar to the Redfield molar ratio of 16 (ca. 13, although the slight N limitation has increased in recent years; Rolff and Elfving 2015), while it is considerably lower in the Baltic Proper (ca. 4), indicating strong N limitation (Savchuk 2018). Diazotrophic primary producers, such as some species of bloom forming cyanobacteria, can bypass this N-limitation by directly fixing N<sub>2</sub>. Satellite images of surface accumulations indicate that these blooms have increased since the 1980s (Kahru and Elmgren 2014), and this internal N loading now exceeds external loadings from rivers and atmospheric deposition in the Baltic proper (Olofsson et al. 2020). Cyanobacterial blooms benefit from denitrification and phosphate release from hypoxic sediments, which exacerbate the N:P imbalance in a 'vicious cycle' (Vahtera et al. 2007). The most recent decade has also seen regular occurrence of cyanobacterial blooms in the Bothnian Sea (Olofsson et al. 2020).

Salinity and temperature are both lower in the Bothnian Sea compared to the Baltic Proper and are the primary factors affecting species distribution, including that of *Cladophora* and *Mytilus*. Predicted increase in temperature and decrease in surface salinity of the Baltic Sea (Räisänen 2017 and references therein) are hence expected to affect organisms, food webs and ecosystems (Andersson et al. 2015a; Vuorinen et al. 2015). Recent studies have shown a decrease in mussel populations over recent decades in the southern Baltic Proper, linked to a changing environment (Franz et al. 2019; Westerborn et al. 2019; Liénart et al. 2020). A shift in dominance from the canopy-forming perennial macrophyte *Fucus* towards opportunistic ephemeral *Cladophora* has been reported since the 1980s in different areas of the Baltic Sea (Kraufvelin and Salovius 2004), likely linked to eutrophication (Kautsky et al. 1986; Råberg 2004; Torn et al. 2006). However, *Fucus* recovery has been observed recently in some areas (Rinne and Salovius-laurén 2020). Nonetheless, higher temperature and declining salinity promote filamentous green algae (Takolander et al. 2017), suggesting climate change will enforce the shift towards ephemeral macrophytes in the Baltic.

Tracing C and N origin in the Baltic Sea is complex, due to multiple interacting sources, especially in the coastal area. For instance, in the Baltic Proper, eutrophication is associated with elevated  $\delta^{15}\text{N}$  values in sediment (Voss et al. 2000) and sewage waters enriched in  $^{15}\text{N}$ , which is traceable in macrophytes (Savage and Elmgren 2004). However, the depleted  $^{15}\text{N}$  signal of synthetic N fertilizers used in agriculture (Bateman and Kelly 2007) can be confounded with the similar signal of diazotrophic cyanobacteria (Rolff 2000), the latter considered an indirect effect of eutrophication (Vahtera et al. 2007). In the Bothnian Sea, the naturally low  $\delta^{15}\text{N}\text{-NO}_3$  from pristine rivers (Voss et al. 2005) should equally be reflected in relatively depleted  $^{15}\text{N}$  baselines. The typically low  $\delta^{13}\text{C}$  of terrestrial carbon from the extensive riverine input in the north (Rolff and Elmgren 2000) is similarly expected to be reflected in a low  $\delta^{13}\text{C}$  baseline in the Bothnian Sea. However, low temperatures and light availability (the latter from brownification) can also result in lower  $\delta^{13}\text{C}$  values for macrophytes (Wiencke and Fischer 1990; Hemminga and Mateo 1996). In the Baltic proper, higher  $\delta^{13}\text{C}$  may reflect eutrophication due to increasing plankton biomass (Oczkowski et al. 2018) with the exception of cyanobacteria (generally low  $\delta^{13}\text{C}$ ; Rolff 2000). In addition, an organism's physiology (e.g. rapid growth, nutritional stress, reproductive stages) can lead to substantial isotope variability in consumers (Doi et al. 2017; Gorokhova 2018). Osmoregulation is an especially N-demanding process for *Mytilus* experiencing low-saline conditions in the Baltic Sea (Tedengren and Kautsky 1987). This likely influences its  $^{15}\text{N}$  fractionation

and hence confounds the dietary origin of the  $\delta^{15}\text{N}$  signal in the mussels (Liénart et al. 2020). To better trace ultimate N sources, the end-member  $\delta^{15}\text{N}$  signal can be measured in source amino acids (e.g. phenylalanine), which show very little  $^{15}\text{N}$  fractionation during assimilation, physiological processes or trophic transfer (McClelland and Montoya 2002) compared to the bulk  $\delta^{15}\text{N}$  signal. Finally, N and P elemental composition is expected to be driven by nutrient background and taxa elemental requirements. The fast-growing algae, which are under little homeostatic control compared to slow growing consumers like mussels (Smaal and Vonck 1997), are expected to reflect basin-specific nutrient conditions, with higher nutrient concentrations in the N limited but nutrient rich Baltic Proper than in the Bothnian Sea. N and P concentrations in mussels might also reflect this difference, but in the low-saline Bothnian Sea this might be confounded by high N requirements during osmotic stress.

In this study, we take advantage of the high temporal resolution of pelagic monitoring data and the archived macroalgae and mussel samples from phytobenthic monitoring in the Baltic Sea to explore whether eutrophication and climate-related changes are mirrored in these key taxa. We retrospectively analyse elemental (C, N and P) and stable isotope ( $\delta^{13}\text{C}$ ,  $\delta^{15}\text{N}$ ) composition of archived samples of the summer growth of the filamentous ephemeral algae *Cladophora* and the slow-growing sessile blue mussel *Mytilus* from three contrasting regions (coastal Bothnian Sea, coastal Baltic Proper and open sea Baltic Proper), spanning 8 to 24 years data depending on region. We first document potential differences and temporal changes in region-specific elemental and isotope baselines, and compare between baselines for algae and mussels. Further, we compare bulk  $\delta^{15}\text{N}$  composition with a smaller data set of  $\delta^{15}\text{N}$  in source amino acids. Then, we test whether it is possible to explain the observed year-to-year variability and long-term trends with environmental and oceanographic data using various statistical approaches. Finally, we link biomass data for both taxa with the stable isotope and environmental data.

We expect elemental and isotope composition of both taxa to reflect the latitudinal gradient in nutrients, with higher values of  $\delta^{13}\text{C}$ ,  $\delta^{15}\text{N}$ , N% and P% in the Baltic proper compared to the Bothnian Sea. We expect *Cladophora* to better reflect nutrient background in its elemental composition than *Mytilus*, due to more homeostatic control of its elemental composition. Finally, we expect *Cladophora* and *Mytilus* to respond differently to environmental and oceanographic variables, and reflect different processes in their ecology and physiology.

## 2. Material And Methods

### 2.1. Study areas and sampling

This study used data from the following study regions: the coastal region Höga Kusten (HK) located in the Bothnian Sea, the coastal archipelago area close to the field station of Askö (A), and the open sea island of Gotland (G), with the latter two sites located in the Baltic Proper (Fig. 1, details Table S1). Within the Swedish marine monitoring program of the phytobenthic community, both the blue mussels *Mytilus* and filamentous green algae *Cladophora* have been sampled once a year at different stations and archived over the periods 1993–2016 for A, 2000–2016 for G, and 2008–2016 for HK. Three replicate samples (20×20 cm quadrates) were collected along land-to-sea transects in late August/early September by SCUBA divers. Samples were oven-dried at 60°C and stored in dark, dry and room temperature (ca. 20°C) conditions. From each year and region, *Mytilus* individuals,  $n = 3$  (G and HK)  $n = 15$  (A), from similar size class (length:  $10.0 \pm 1.5$  mm, mean  $\pm$  sd; Table S1) from 5 m depth at the most exposed station in each region (two stations at HK to allow  $n = 3$  per year; Fig. 1), were selected for biometric and chemical analyses. *Cladophora* material (a few grams homogenised dry weight) from 1 meter depth was selected for chemical analysis for three to six stations per region (Fig. 1). The rationale behind using several stations within each region for *Cladophora* was to avoid variability from local nutrient conditions (such as bird guano on a particular rock), whereas one station was deemed sufficient for mussels, which actively filter-feeds large amounts of water.

Temperature (°C), salinity, dissolved inorganic nitrogen and phosphorus (DIN, DIP,  $\mu\text{mol L}^{-1}$ ), total nitrogen and phosphorus (total N, total P,  $\mu\text{mol L}^{-1}$ ; i.e. includes dissolved inorganic, dissolved organic, and particulate fractions), and the

phytoplankton community were measured by the Swedish national monitoring program for the nearby pelagic ecosystem: the station C3 close to Höga Kusten, station B1 close to Askö island in Stockholm's archipelago and the open sea station BY31 north of Gotland island (Fig. 1, Table S1). For more details about sampling and analytical methods, see supplemental material Table S1, Andersson et al. (2015b) and Liénart et al. (2020). All environmental and phytoplankton community data are available at <http://www.smhi.se> (Marine environmental monitoring data - SHARK database). Surface terrestrial total organic carbon transport (TOC, total loadings in tons) for each watershed in Sweden is measured monthly within the freshwater monitoring program "river mouths" (chemical analyses) and is available at <http://webstar.vatten.slu.se/db.html> (HAVET 2015/2016).

## 2.2. Elemental and isotope analysis

Dry ground material from both *Cladophora* and *Mytilus* soft tissue (from the same size class, shell not included) were used for elemental carbon, nitrogen and phosphorus (% of C, N, P per dry weight), bulk carbon and nitrogen isotope ( $\delta^{13}\text{C}$ ,  $\delta^{15}\text{N}$ ) and amino-acid- $\delta^{15}\text{N}$  measurements (AA- $\delta^{15}\text{N}$ ). Individual specimens of *Mytilus* were used for C and N elemental and isotope measurements and P % was measured individually in different specimens, since the mussels were too small for all analyses in the same individual (soft tissue was on average  $2.1 \pm 1.5$  mg in mussels in this size range; Table S1). Phosphorus in *Cladophora* was only measured for 4 of the 6 stations at A (not measured for from Lac and StA) and 3 of the 4 stations at HK (not measured for Dön). Amino-acid- $\delta^{15}\text{N}$  analysis was performed on pooled *Mytilus* (ca. 5 individuals per region and year).

Phosphorus analyses of individual mussels were performed at the Department of Ecology, Environment and Plant Sciences (Stockholm, Sweden) using a Alpkem SFA system to analyse phosphate (SS-EN ISO 15681-2:2018), after combustion and persulfate digestion, following Larsson et al. (2001). C and N elemental and bulk stable isotopes were measured at the Center for Physical Science and Technology (Vilnius, Lithuania) with a Flash EA 1112 Series Elemental Analyzer (Thermo Finnigan) connected to a DeltaV Advantage Isotope Ratio Mass Spectrometer (Thermo Fisher).

Amino-acid- $\delta^{15}\text{N}$  analysis of *Mytilus* was conducted at the Center for Physical Science and Technology (Vilnius, Lithuania) and details are presented in supplemental material. In brief, the extraction and derivatization of amino acids were performed following the method described in Ledesma et al. (2020), then analysed by GC-C-IRMS with a Trace GC Ultra Gas Chromatograph (Thermo scientific) coupled to a Delta Advantage Isotope Ratio Mass Spectrometer via GCC III combustion interface (ThermoFinnigan). *Cladophora* amino-acid- $\delta^{15}\text{N}$ , which had a lower N content, was analysed at the University of California Davis Stable Isotope Facility (UC Davis) following the method described on <https://stableisotopefacility.ucdavis.edu/gcamino.html> (details in suppl. material).

All isotope data are expressed using the conventional delta notation:  $\delta^{13}\text{C}_{\text{sample}}$  or  $\delta^{15}\text{N}_{\text{sample}} = [(R_{\text{sample}}/R_{\text{standard}})-1]$ , where  $R = {}^{13}\text{C}/{}^{12}\text{C}$  or  ${}^{15}\text{N}/{}^{14}\text{N}$ , with per mil deviation (‰) from international standards, Vienna Pee Dee belemnite for  $\delta^{13}\text{C}$  and atmospheric  $\text{N}_2$  for  $\delta^{15}\text{N}$ . External and internal standards were analysed as references within each batch of samples (details in suppl. material). Analytical uncertainties were  $< 0.15\text{‰}$  and  $< 0.20\text{‰}$  for  $\delta^{13}\text{C}$  and  $\delta^{15}\text{N}$  respectively and  $< 0.30\text{‰}$  for AA- $\delta^{15}\text{N}$ . The overall analytical precision was 0.9% and 0.2% for elemental C and N respectively.

In total, 239 *Cladophora* and 507 *Mytilus* samples were analysed for C and N elemental and bulk isotope ratio, 150 *Cladophora* and 147 *Mytilus* samples for phosphorus, and 9 *Cladophora* and 12 *Mytilus* samples for amino acid- $\delta^{15}\text{N}$ .

## 2.3. Data analyses

### 2.3.1. *Mytilus* and *Cladophora* variables and population data

For the individual *Mytilus* used for isotope analyses, the Condition Index ( $\text{CI}_{\text{Mytilus}} = \text{dry weight soft tissue (g)} / \text{dry weight shell (g)} \times 100$ ) was calculated as an indicator of mussels' health status (e.g. Filgueira et al. 2013; Irisarri et al. 2015). The N:P ratio of both taxa ( $\text{N:P}_{\text{Cladophora}}$ ,  $\text{N:P}_{\text{Mytilus}}$ ) was calculated to be compared to Redfield ratio in the water.

For each station of the three regions (Fig. 1), and for each year, i) *Cladophora* total biomass (g dry weight per m<sup>2</sup>) from ca. 1 meter depth, ii) *Mytilus* total biomass (g dry weight including shells per m<sup>-2</sup>) and abundance (individual per m<sup>2</sup>), as well the ratio between the two (Bm:Ab<sub>Mytilus</sub>, mg dry weight per individual, a proxy for average mussel size in the population), were calculated for all size classes (from juveniles ≥ 1 mm to bigger mussels > 10 mm, only a few individuals had a shell length exceeding 20 mm, Åkermark et al. in prep) at ca. 5 m depth. Calculations for each region (average of stations) were based on geometric mean for the total biomass of both taxa and the Bm:Ab<sub>Mytilus</sub> ratio, to avoid influence from extreme values, and on the median for *Mytilus* abundance.

## 2.3.2. Environmental variables

For each station, environmental data were first integrated over 0–10 m depth (average) for each sampling date, then averaged per month (linear interpolation was performed for missing sampling dates or months). The average values per period were then calculated: the annual mean (January to August 31st, i.e. approximate date of biota sampling each year) for temperature, salinity, total N and P and the winter mean (January-February, i.e. reliable period to measure nutrient concentrations and reflect the general conditions of each region) for DIN and DIP concentrations (Table S1). The DIN:DIP ratio in the water (mol:mol) was calculated for each year based on winter concentrations. The maximum summer temperature (T<sub>max</sub>) was considered over the period June-August for the Baltic Proper stations and July-August for the Bothnian Sea (Table S1). The total biovolume (mm<sup>3</sup> L<sup>-1</sup>) of phytoplankton community (total Phyto.) integrated over 0–10 m depth (multiplied by 2 at stations B1 and BY31 to adjust for the tube sampling depth of 0-20m compared to the 0–10 at C3, Olofsson et al. 2020) was calculated over the productive period (March-August, see details Table S1). In addition, and over the same period, the biovolume of four groups representing most of the phytoplankton community biomass (diatoms, dinoflagellates, cyanobacteria and the ciliate *Mesodinium rubrum*) were recalculated as an integrated sum (area under the curve (AUC) linear interpolation), following Liénart et al. (2020) (see details Table S1). A lag in the productive period was considered for the northern station (April-August). Summer AUC values, for only cyanobacteria, were also calculated to be later compared with *Cladophora* variables. Yearly averages of total organic carbon loadings (TOC<sub>terr</sub>, tons) were calculated from the different watersheds of each region (Table S1). The average day of the year the shift in water temperature from 8 to 10–12°C occurred (i.e. temperature rise triggering spawning, Kautsky pers. com.) was calculated for each region (T<sub>shift</sub>, in Julian days) and used as a proxy of climate change (with this shift supposedly occurring earlier in recent years). Finally, to capture the variations in the Ocean-Atmosphere Regime of the Baltic Sea (i.e. large-scale climatic index related to the North Atlantic Oscillation), the Baltic Sea Index (BSI) was calculated according to Lehmann et al. (2002).

## 2.4. Statistical analysis

Data treatment and statistical analysis were performed using R free software (R Core Team (2020). R: A language and environment for statistical computing. R Foundation for Statistical Computing, Vienna, Austria. <https://www.R-project.org/>, version 4.0.3 (2020-10-10)), except for the DistLM models, which were performed in PERMANOVA+ of PRIMER version 6 (Anderson et al. 2008). For all statistical univariate tests, critical *p*-value was set to 0.05.

### 2.4.1. Spatial variability and temporal trends

Local variability in elemental and isotope composition of *Cladophora* was investigated within each region prior to subsequent analyses. Unidirectional trends in time series using Mann-Kendall tests (details below) were explored for the individual stations within a region. Potential station effect over the entire time period was tested with Kruskal-Wallis test followed by Bonferroni corrected Mann-Whitney pairwise comparison tests. Since little difference among stations was found (see results 3.1.1.), annual mean per region based on the 3 to 6 stations was computed for each variable, to be used in subsequent analyses.

For all biological and environmental variables and all regions, time-series (using annual mean values) were tested for unidirectional trend using Mann-Kendall tests. Autocorrelation was checked (acf(), {stats}), and if required, a modified version of the test for autocorrelated time series was applied (mmkh3lag(), {modifiedmk} package, version 1.5.0, allowing

autocorrelations). Potential differences in absolute values of the various biological endpoints among regions were tested over the last 9 years of each time period (Höga Kusten is only 9 years long), with Kruskal-Wallis test followed by Bonferroni corrected Mann-Whitney pairwise comparison tests.

## 2.4.2. Correlations

For environmental, and some of the biological, variables (% C, N, P, N:P<sub>Cladophora</sub>), correlations were evaluated with Spearman's rank correlation. For stable isotope and biometric data on *Mytilus* ( $\delta^{13}\text{C}$ ,  $\delta^{15}\text{N}$ , Cl<sub>Mytilus</sub>), correlations were evaluated with Pearson's correlation. Correlations were evaluated: i) among biological variables of the same taxa and region, ii) for each unique variable of the same taxa among regions over the same time series length iii) for each unique variable between *Mytilus* and *Cladophora* within each region and iv) among environmental variables for each region.

In order to summarize the major patterns of variation among the different regions, principal component analyses (PCA, scaled data) were performed for i) elemental and isotope composition of *Cladophora* and *Mytilus* and ii) environmental data.

## 2.4.3. Linking biological datasets with environmental data

To test which of the environmental variables (11 for *Cladophora*, 15 for *Mytilus*, Table S2) influenced the combined dataset of elemental and isotope composition of *Cladophora* or *Mytilus*, distance-based linear models were used (DistLM, Euclidean distances of normalized data, forward selection of explanatory variables based on Akaike information criterion). The final DistLM model was plotted as a redundancy analysis.

Partial least squares regression (PLSR) were used to model the relationship between a single response variable in each taxa ( $\delta^{15}\text{N}$ ,  $\delta^{13}\text{C}$ , N%, P%) or the population biomass (and for *Mytilus*, the abundance and Bm:Ab<sub>Mytilus</sub>) with the environmental and phytoplankton explanatory variables (11 to 17 predictors, Table S2). PLSR analyses were performed on mean-centred and variance-standardized data, with models optimized to two components (as detailed in Lienart et al. 2020). Selection and removal of predictors were performed stepwise i) according to the variable of importance for projection (VIP) scores values (with a cut-off of 0.8 Wold et al. (2001) extended to 0.9 when needed for more parsimonious models i.e.  $\leq 7$  predictors) and ii) trying to maximize both R<sup>2</sup>Q (indicates model predictive capacity) and R<sup>2</sup>Y (explanatory capacity, analogous to coefficient of determination in regression analysis, R<sup>2</sup>X is the explained variance). Quality of the model was evaluated based on both explanatory R<sup>2</sup>Y > 0.6 and predictive R<sup>2</sup>Q > 0.4 capacities. Standardized regression coefficients were calculated for each predictor from the two-component model to ascertain the significance of environmental factors explaining and predicting the variance in response variables. PLSR analyses were performed using a modified version of the {pls} R package (v. 2.7-0, August 2018) as detailed in Liénart et al. (2020). The rationales for including predictors in the different models are presented Table S2.

In order to test if the N:P of the biota was linked to the DIN:DIP in the water of each region over time, linear models were applied for each taxon (lm(), allowing the interaction region x N:P water). Variability in N:P<sub>Cladophora</sub> was also investigated locally (4 stations, Fur, Str, Jus, Iss) for our longest time series only (A), using distance to the shore (in km from an arbitrary runoff point selected with regard to the agricultural landscape occupying the bay and its position relative to the stations), and compared with the local DIN:DIP in the water (inner station, sö28 and outer station sö25; 2004–2016 August only; Fig. 1).

## 3. Results

### 3.1. Elemental and isotope baselines

#### 3.1.1. Comparison between *Cladophora* within regions

There were no significant differences in *Cladophora*  $\delta^{13}\text{C}$  and  $\delta^{15}\text{N}$  between stations in any of the regions, although  $\delta^{13}\text{C}$  between Bön and Sjä at Höga Kusten was marginally significant ( $p = 0.05$ ; Table S3, Fig. S1). There were no significant

temporal trends in any of *Cladophora* elemental and isotope variables over time (Table S4). Elemental composition differed between some stations of Askö archipelago and Gotland (Table S3). Thus, mean values for *Cladophora*  $\delta^{13}\text{C}$  and  $\delta^{15}\text{N}$  and C, N and P % were calculated, and used in subsequent analyses.

### 3.1.2. Comparisons of absolute values among taxa and regions

Regardless of region, the % P and N were higher in the mussels (N:  $9.5 \pm 1.0$  %, P:  $0.8 \pm 0.1$  %) than in the green algae (N:  $1.9 \pm 0.4$  %, P:  $0.1 \pm 0.04$  %), and  $\delta^{13}\text{C}$  were higher for *Cladophora* ( $15.9 \pm 1.8$ ‰) than *Mytilus* ( $-22.3 \pm 0.8$ ‰).  $\delta^{15}\text{N}$  was generally higher for *Mytilus* ( $5.1 \pm 1.3$ ‰), except for *Cladophora* from Askö, which showed high values comparable to the mussels at this site ( $5.8 \pm 1.2$ ‰), but was lower in the other regions (ca.  $2.0 \pm 1.5$ ‰) (Fig. 2). Both taxa had significantly higher  $\delta^{15}\text{N}$  values from the Askö archipelago area compared to the other regions (Fig. 2, Fig. S2, Table S5). *Cladophora*  $\delta^{13}\text{C}$  was lower at Höga Kusten and *Mytilus*  $\delta^{13}\text{C}$  was higher at Gotland compared to the other regions (Fig. 2, Fig. S2, Table S5). For both taxa, N % and N:P ratio did not differ between the regions and P % was generally lower at Gotland compared to Höga Kusten (Fig. 2, Fig. S2, Table S5). The condition index of *Mytilus* ( $CI_{Mytilus}$ ) was significantly higher for the mussels of Höga Kusten than for the Baltic Proper, and Askö archipelago was significantly lower than Gotland (Fig. 2, Fig. S2, Table S5). Within each region,  $\delta^{13}\text{C}$  and  $\delta^{15}\text{N}$  were never correlated for the mussels nor algae (Table S6). *Cladophora*  $\delta^{13}\text{C}$  and N % were positively correlated at Askö archipelago and negatively correlated at Gotland.  $\delta^{13}\text{C}$  and N:P<sub>*Cladophora*</sub> were positively correlated at the coastal stations Askö archipelago and Höga Kusten, while negatively correlated at Gotland. *Mytilus* C and N % were positively correlated over time for the 3 regions (Table S6).

### 3.1.3. Time trends and correlations among taxa and regions

Over time, *Mytilus*  $\delta^{13}\text{C}$  and  $\delta^{15}\text{N}$  at Askö ( $\tau = -0.37$ ,  $p = 0.01$ ,  $\tau = -0.41$ ,  $p = 0.005$  respectively) and N % at Gotland ( $\tau = -0.50$ ,  $p = 0.01$ ) were significantly decreasing, while no patterns in isotopes could be identified for the shorter time series (Table S7, Fig. 2). There was no significant trend for any of *Cladophora* variables. *Mytilus*  $\delta^{13}\text{C}$  was positively correlated between the two coastal stations of Askö archipelago and Höga Kusten ( $r = 0.82$ ,  $p = 0.01$ ) and between the two stations of the Baltic Proper (Gotland and Askö archipelago,  $r = 0.59$ ,  $p = 0.02$ ; Table S8). *Mytilus* N % was positively correlated between Gotland and Höga Kusten ( $\rho = 0.78$ ,  $p = 0.02$ ; Table S8, no correlations between regions for *Cladophora* variables).

### 3.1.4. Correlation between taxa within regions

*Cladophora* and *Mytilus*  $\delta^{13}\text{C}$  were positively correlated at Gotland ( $r = 0.65$ ,  $p = 0.01$ ), and for their  $\delta^{15}\text{N}$  values in the Askö archipelago ( $r = 0.41$ ,  $p = 0.04$ ), while no significant correlation was observed at Höga Kusten (please note  $n = 9$ ; Table S9).

### 3.1.5. $\delta^{15}\text{N}$ in amino acids for both taxa

Regardless of region, *Mytilus* had generally negative  $\delta^{15}\text{N}$  values of the source amino acid Phenylalanine ( $\delta^{15}\text{N-Phe}$ ) compared to more positive values for *Cladophora* (Fig. 3). There was a significant correlation between bulk  $\delta^{15}\text{N}$  and  $\delta^{15}\text{N-Phe}$  for both taxa (*Mytilus*:  $p = 0.028$ ,  $\rho = 0.61$ ; *Cladophora*:  $p = 0.008$ ,  $\rho = 0.83$ , Fig. 3). Between regions, *Mytilus*  $\delta^{15}\text{N-Phe}$  was lowest at Gotland ( $-2.9 \pm 1.6$ ‰) and Höga Kusten ( $-1.9 \pm 0.4$ ‰) and higher at the Askö archipelago ( $-0.7 \pm 2.0$ ‰). *Cladophora*  $\delta^{15}\text{N-Phe}$  was lowest at Höga Kusten ( $-0.7 \pm 0.03$ ‰), intermediate at Gotland ( $1.1 \pm 3.5$ ‰), and highest for the Askö archipelago area ( $4.6 \pm 3.4$ ‰) (Fig. S3).

## 3.2. Population biomass and abundance

The biomass of *Cladophora* was on average similar at all regions (A:  $7.7 \pm 7.6$  g m<sup>-2</sup>, G:  $6.6 \pm 5.4$  g m<sup>-2</sup>, HK:  $5.6 \pm 4.7$  g m<sup>-2</sup>; Fig. 4, Table S7), and there was no temporal trend over time nor correlation between regions (Table S7 and S8). *Mytilus* biomass was high at Askö archipelago stations ( $453 \pm 163$  g m<sup>-2</sup>), about four times lower at Gotland ( $129 \pm 43$  g m<sup>-2</sup>), and 100 times lower at Höga Kusten ( $4 \pm 3$  g m<sup>-2</sup>, Fig. 4, Table S7). *Mytilus* abundance was ca. 100 times higher in the Baltic Proper (Askö archipelago:  $12478 \pm 6433$  individual m<sup>-2</sup>, Gotland:  $21939 \pm 12020$  individual m<sup>-2</sup>) than in the Bothnian Sea

(HK:  $218 \pm 140$  individual  $m^{-2}$ ; Fig. S4, Table S5). Accordingly, the average mussel size of the population ( $Bm:Ab_{Mytilus}$ ) was the highest at the coastal stations (Askö archipelago:  $36.4 \pm 17.9$  mg individual $^{-1}$ ; Höga Kusten:  $27.6 \pm 20.8$  mg individual $^{-1}$ ), and considerably lower at the open sea station of the Baltic Proper (Gotland:  $6.8 \pm 2.7$  mg individual $^{-1}$ ; Fig. S4, Table S5). Over time, *Mytilus* biomass significantly decreased in Askö archipelago (average of 6 stations), mussels' abundance significantly decreased at Höga Kusten (average of 4 stations), and the average mussel size of the population decreased in the Baltic Proper (significant for Gotland, marginally significant ( $p = 0.06$ ) for Askö archipelago, Table S7, Fig. S4).

### 3.3. Environmental data

C3 in the Bothnian Sea was characterized by high total organic carbon loadings ( $TOC_{terr}$ ), low salinity and water temperature, low total nitrogen (N) and phosphorus (P), and low dissolved inorganic phosphorus (DIP) concentrations (Fig. 5, Fig. S5). Generally, B1 and BY31, in the coastal and open Baltic Proper respectively, had higher salinity, total and dissolved N and P concentrations and total phytoplankton biovolumes (total Phyto.) compared to C3 (Fig. 5, Fig. S5). B1 was characterized by higher concentrations of dissolved inorganic N (DIN), while BY31 had more dinoflagellates,  $N_2$ -fixing cyanobacteria and larger phytoplankton biovolumes (Fig. 5, Fig. S5). Over time (Fig. S5, Table S10), C3 showed a significant decrease in DIN:DIP. Both B1 and BY31 showed a significant increase in total P and significant decrease in temperature shift ( $T_{shift}$ ), indicating that the rapid temperature rise from 8 to 10–12 °C is now occurring earlier in the year in the Baltic Proper. Total N and phytoplankton biomass, especially dinoflagellates, significantly increased at BY31. DIN, DIN:DIP and the ciliate *Mesodinium rubrum* significantly decreased and  $TOC_{terr}$  significantly increased at B1. Environmental variables were rarely correlated (Table S11).

### 3.4. Explaining elemental, isotope and population changes

#### 3.4.1. Elemental and isotope baselines

Generally, elemental and isotope composition of *Cladophora* ( $R^2_{adj.} = 0.35$ ) and *Mytilus* ( $R^2_{adj.} = 0.31$ ) were associated in the DistLM analyses with 5 environmental variables, of which three were the same (DIN, salinity,  $T_{max}$ , Fig. 6, Table S12). Higher  $\delta^{13}C$  values in *Cladophora* were linked to high salinities and maximum water temperatures in summer ( $T_{max}$ ). For *Mytilus*, high  $\delta^{13}C$  was linked to high dinoflagellates biovolumes. Higher  $\delta^{15}N$  values were linked to high dissolved inorganic nitrogen (DIN) in both *Cladophora* and *Mytilus*, driven by the high values in samples from the coastal station of Askö archipelago.

When isotope and elemental response variables were tested separately using PLSR across regions (Table 1), the  $\delta^{15}N$  models of both taxa met the Lundstedt criteria (predictive capacity  $R^2Q > 0.4$ ; Lundstedt et al. 1998). In line with DistLM models, high values of  $\delta^{15}N$  for both taxa were explained by high DIN. High  $\delta^{15}N$  in *Cladophora* was generally linked to high nutrient levels (DIP, total N) and to an earlier warming of waters ( $T_{shift}$ ). Large blooms of  $N_2$ -fixing cyanobacteria were linked to low  $\delta^{15}N$  of *Mytilus*. The condition index ( $CI_{Mytilus}$ ) was also included as a predictor in the mussel's  $\delta^{15}N$  model, with better condition (high  $CI_{Mytilus}$ ) linked to lower  $\delta^{15}N$ . In turn, *Mytilus* condition was best explained by  $\delta^{15}N$  (negative relationship). It was furthermore linked to the Baltic Sea Index, a proxy for global climate change, and to earlier warming of water ( $T_{shift}$ ), which negatively affected the mussels' condition. Higher  $TOC_{terr}$  was associated with higher  $CI_{Mytilus}$ . High  $\delta^{13}C$  for *Cladophora* was linked to high water temperature (annual and summer maximum  $T_{max}$ ), high phosphorus concentrations (dissolved inorganic), and high total organic carbon ( $TOC_{terr}$ ), the latter a proxy for low light penetration (Table S2). Low  $\delta^{13}C$  in *Mytilus* was linked to high DIN, high  $TOC_{terr}$ , a proxy for food availability (bearing a low  $\delta^{13}C$  signal, Table S2), and to higher salinities as well as greater total N and P. The models for elemental content for both taxa generally had low predictive and explanatory performance. High N % in *Cladophora* was linked to high nutrients (DIN, DIP), and to low phytoplankton bloom (more light availability, a proxy for lower competition for nutrients, Table S2). In the mussels, high N % was linked to higher  $CI_{Mytilus}$  and lower water temperatures, as well as earlier warming of water. High P % in *Cladophora* was linked to high summer water

maximum temperature, low total phytoplankton bloom and low  $\text{TOC}_{\text{terr}}$  loadings (higher light availability). *Mytilus* P % was positively linked to DIN and to proxies for diet quality (diatoms and dinoflagellates).

Table 1

Results of the PLSR models for the 6 *Cladophora* and 8 *Mytilus* response variables tested (in white: individual level, in dark grey: population level).  $R^2Y$  is the model explanatory capacity,  $R^2Q$  is the model predictive capacity,  $R^2X$  is the explained variance. Models with high prediction capacity according to Lundstedt evaluation criteria (Lundstedt et al. 1998;  $R^2Y > 0.6$  and  $R^2Q > 0.4$ ) are in bold. Shaded grey cells are predictors with negative influence. The '-' sign means no additional predictors. Predictors are ranked by importance based on absolute value of regression coefficient (in italics).  $CI_{Mytilus}$ : condition index, Abund.: abundance, Temp.: water temperature,  $T_{max}$ : maximum summer water temperature,  $T_{shift}$ : water temperature shift, DIP and DIN: dissolved inorganic nitrogen or phosphorus,  $TOC_{terr}$ : total organic carbon loadings, Tot. Phyto.: total phytoplankton biomass, NfixCyb.:  $N_2$ -fixing cyanobacteria, Diat.: diatoms, Dino.: dinoflagellates, BSI: Baltic Sea Index.

Response variable		Model evaluation parameters			Predictors (reg. coefficients)						
		$R^2Y$	$R^2Q$	$R^2X$	1	2	3	4	5	6	7
$\delta^{13}C$	<i>Cladophora</i>	0.4	0.3	0.8	$T_{max}$	Temp.	DIP	Total P	Salinity	$TOC_{terr}$	Total N
					<i>0.92</i>	<i>0.32</i>	<i>0.14</i>	<i>-0.09</i>	<i>-0.08</i>	<i>0.06</i>	<i>-0.05</i>
$\delta^{15}N$		<b>0.6</b>	<b>0.5</b>	<b>0.9</b>	<b>DIN</b>	<b>DIP</b>	<b><math>T_{shift}</math></b>	<b>Total N</b>	<b>Total P</b>	<b>Salinity</b>	-
					<i>0.92</i>	<i>0.29</i>	<i>-0.27</i>	<i>0.24</i>	<i>-0.07</i>	<i>0.04</i>	
N %		0.3	0.2	0.8	DIN	DIP	Tot. Phyto	Total N	-	-	-
					<i>0.12</i>	<i>0.08</i>	<i>-0.05</i>	<i>0.02</i>			
P %		0.3	0.2	0.8	Tot. Phyto	$T_{max}$	Salinity	$TOC_{terr}$	-	-	-
					<i>-0.01</i>	<i>0.007</i>	<i>0.004</i>	<i>-0.004</i>			
Biomass		0.2	0.0	0.7	$\delta^{15}N$	BSI	$\delta^{13}C$	Total N	DIP	-	-
					<i>1.26</i>	<i>-1.25</i>	<i>-0.93</i>	<i>0.77</i>	<i>0.61</i>		
$\delta^{13}C$	<i>Mytilus</i>	0.4	0.3	0.9	DIN	Total P	Salinity	$TOC_{terr}$	Total N	-	-
					<i>-0.31</i>	<i>0.11</i>	<i>0.10</i>	<i>-0.08</i>	<i>0.02</i>		
$\delta^{15}N$		<b>0.6</b>	<b>0.5</b>	<b>0.8</b>	<b>DIN</b>	<b><math>CI_{Mytilus}</math></b>	<b>NfixCyb.</b>	-	-	-	-
					<i>0.59</i>	<i>-0.49</i>	<i>-0.28</i>				
N %		0.2	0.1	0.8	$CI_{Mytilus}$	$T_{shift}$	$T_{max}$	Total N	-	-	-
					<i>0.35</i>	<i>-0.18</i>	<i>-0.08</i>	<i>0.01</i>			
P %		0.3	0.2	0.7	DIN	Dino.	Total P	Diat.	Salinity	-	-
					<i>0.025</i>	<i>-0.017</i>	<i>-0.016</i>	<i>0.014</i>	<i>-0.013</i>		
$CI_{Mytilus}$		0.4	0.3	0.7	$\delta^{15}N$	BSI	Total N	$T_{shift}$	$TOC_{terr}$	Salinity	-
					<i>-0.005</i>	<i>0.004</i>	<i>-0.003</i>	<i>0.002</i>	<i>0.002</i>	<i>-0.001</i>	
<b>Biomass</b>		<b>0.7</b>	<b>0.7</b>	<b>0.8</b>	<b><math>\delta^{15}N</math></b>	<b>DIN</b>	<b>DIP</b>	<b>Total N</b>	<b><math>TOC_{terr}</math></b>	-	-
					<i>75</i>	<i>68</i>	<i>41</i>	<i>29</i>	<i>-24</i>		

Response variable	Model evaluation parameters			Predictors (reg. coefficients)						
Abund.	0.6	0.5	0.8	DIN	$\delta^{13}\text{C}$	Total P	Salinity	TOC <sub>terr</sub>	-	-
				-2638	2635	2320	2238	-1827		
Bm:Ab	0.6	0.5	0.8	$\delta^{15}\text{N}$	NfixCyb.	DIN	-	-	-	-
				0.007	-0.007	0.005				

The simpler linear models testing for stoichiometric relationship between the elemental ratio N:P of the biota and water between different regions did not show any effect for *Mytilus*. However, *Cladophora* N:P was explained by region-specific differences in water nutrient DIN:DIP ratio (Fig. S6). These results are supported by a local dataset from Askö archipelago, where N:P<sub>Cladophora</sub> is low in the inner station (Fur) compared to high values for the outer archipelago (Iss, significantly higher than the inland stations), with this pattern also observed for the DIN:DIP in the water between these two locations (Fig. S7).

### 3.4.2. Linking isotopes, elements and environmental data to population biomass

Only the *Mytilus* population models met the Lundstedt criteria (predictive capacity  $R^2Q > 0.4$ ) and had high explanatory power ( $R^2Y \geq 50\%$ ; Table 1). High *Mytilus* biomass was linked to high  $\delta^{15}\text{N}$ , high nutrient concentrations (DIN, DIP, total N) and to low TOC<sub>terr</sub>. The abundance of mussels was negatively linked to DIN and TOC<sub>terr</sub>, but positively associated with total P and salinity. Smaller mean size for mussels (Bm:Ab<sub>Mytilus</sub>) was linked to lower  $\delta^{15}\text{N}$  of the mussels, to lower DIN and to higher N<sub>2</sub>-fixing cyanobacterial blooms.

## 4. Discussion

Our study documents large-scale and long-term patterns in elemental and isotope baselines in the ephemeral filamentous macroalgae *Cladophora* spp. and the suspension-feeding blue mussel *Mytilus* sp., two key-taxa from the Baltic Sea. Observed differences in elemental and isotope composition were statistically linked to environmental pelagic monitoring data. Overall, the  $\delta^{13}\text{C}$  baseline differed between algae and mussels, following a latitudinal gradient for the algae, while it instead differed between the coastal and open sea environment for mussels. Nonetheless, mussels from the different regions had similar temporal development in  $\delta^{13}\text{C}$ , suggesting a global driver influencing  $\delta^{13}\text{C}$  dynamics in the pelagic ecosystem. The  $\delta^{15}\text{N}$  baseline was more region-specific, and  $\delta^{15}\text{N}$  in the source amino acid Phenylalanine ( $\delta^{15}\text{N}$ -Phe) revealed clear differences between mussels and algae regarding ultimate N source, not always visible in bulk  $\delta^{15}\text{N}$ . Elemental composition only differed for both taxa between locations for P %, which was lower at the open sea station. *Cladophora* N:P reflected regional nutrient levels in the water, while *Mytilus* P % was linked to food quality. Finally, at population levels, *Mytilus* biomass and abundance were, as expected, lower in the Bothnian Sea due to low salinity, but was however also related to food quality such as terrestrial organic carbon and cyanobacterial bloom.

### 4.1. Spatial $\delta^{13}\text{C}$ pattern differs among taxa

The  $\delta^{13}\text{C}$  baseline for *Cladophora* followed a latitudinal pattern, with most depleted values in the north. This pattern was mainly explained by physical variables: the low  $\delta^{13}\text{C}$  in the algae from Höga Kusten, compared with algae from the Baltic proper, was linked to low water temperature and terrestrial loading, which was our proxy for light penetration but might also indicate dissolved inorganic carbon with a different endmember  $\delta^{13}\text{C}$  value. Light and temperature are known to drive growth and C uptake in macrophytes, thereby influencing their  $\delta^{13}\text{C}$  values. Enriched  $^{13}\text{C}$  (less negative  $\delta^{13}\text{C}$ ) is associated with enhanced photosynthetic activity in warm areas like the tropics, experiencing high irradiance, compared to temperate and polar regions (Wiencke and Fischer 1990; Hemminga and Mateo 1996; Stepien 2015). *Cladophora*  $\delta^{13}\text{C}$  was further linked to

phosphorus levels in the water (DIP), which likely influence its growth condition and hence  $\delta^{13}\text{C}$ . In limnic systems, P is the limiting factor for *Cladophora* growth (Howell 2018 and references therein) but, to our knowledge, no studies have tested whether N or P limit *Cladophora* growth in the Baltic Sea.

The  $\delta^{13}\text{C}$  of *Mytilus* showed no latitudinal pattern, but instead differed between coastal areas and open sea. Similarly depleted  $^{13}\text{C}$  values were observed for the two coastal stations (Askö archipelago and Höga Kusten), despite them being situated in different basins. In the statistical models, low  $\delta^{13}\text{C}$  was linked to higher eutrophication (dissolved inorganic nitrogen: DIN) and total organic carbon loadings from land ( $\text{TOC}_{\text{terr}}$ ), and to lower salinity. Filter-feeders opportunistically feed on terrestrial or organic particles from resuspended old sediment, both bearing a low  $\delta^{13}\text{C}$  signal (Rolff and Elmgren 2000; Voss et al. 2000), in shallow areas or at the vicinity of river mouths, which is mirrored in their tissues (Lefebvre et al. 2009; Pernet et al. 2012; Briant et al. 2018). In a recent study comparing the isotope signal of benthic and pelagic food web components in different sub-basins of the Baltic Sea, Kiljunen et al. (2020) found a progressive north to south  $^{13}\text{C}$  enrichment pattern in both benthic and pelagic baselines, supposedly influenced by the amount of allochthonous organic material from freshwater inflows. However, it is less likely that the low  $\delta^{13}\text{C}$  signal of *Mytilus* from the coastal station of Askö archipelago, nearly identically to Höga Kusten, can be explained by temporally similar  $\text{TOC}_{\text{terr}}$  inputs since total organic carbon loadings are 10-fold lower in the archipelago area compared to Höga Kusten. Other processes are likely involved, and the significant correlation between  $\delta^{13}\text{C}$  in mussels from Askö archipelago and Gotland suggests a global driver influencing the pelagic ecosystem. Despite the correlation over time, higher  $\delta^{13}\text{C}$  for *Mytilus* from the open sea region Gotland reflects a more marine signal, less influenced by terrestrial runoff (Rolff and Elmgren 2000). Another contributing variable to the higher  $\delta^{13}\text{C}$  in *Mytilus* from Gotland could be greater eutrophication of the open Baltic Proper. The overall Baltic Sea is classified as 'problem areas' with eutrophication status rated as mostly poor for the Baltic Proper compared with moderate to poor for the Bothnian sea according to the HELCOM Eutrophication Assessment Tool, which could result in  $^{13}\text{C}$  enriched values due to high plankton biomass (Oczkowski et al. 2018).

## 4.2. Common $\delta^{13}\text{C}$ temporal trends of biota may reflect global environmental changes

Over time, our longest dataset (1993–2016) from Askö archipelago in the coastal Baltic Proper, revealed a significant decrease in *Mytilus*  $\delta^{13}\text{C}$  as reported in Lienart et al. (2020). A similar decrease in *Mytilus*  $\delta^{13}\text{C}$  was also demonstrated from the same time period in Kvädöfjärden, a coastal station 100 km south of Askö archipelago (Ek et al. 2021). However, Kvädöfjärden time series was longer (starting in 1981), and there was no evident decrease when considering the nearly 4 decades. The nearly identical temporal variation (and absolute values) in  $\delta^{13}\text{C}$  for mussels from Askö archipelago and Höga Kusten, and the positive correlation over time in  $\delta^{13}\text{C}$  for *Mytilus* from Kvädöfjärden, Askö archipelago and Gotland, suggest a large-scale effect on  $\delta^{13}\text{C}$  values. Furthermore, mussels and algae  $\delta^{13}\text{C}$  were positively correlated at Gotland and Askö archipelago ( $p < 0.08$  in both cases). This large-scale similarity in  $\delta^{13}\text{C}$  over time may hence reflect global or at least northern hemisphere changes not included in our statistical approach. The worldwide decrease in  $\delta^{13}\text{C}$  of atmospheric  $\text{CO}_2$  as a result of global anthropogenic activities (e.g. fossil fuels use and deforestation; referred to as the Suess effect; Gruber et al. 1999; Quay et al. 2007), has significantly affected marine biota over recent decades (Schloesser et al. 2009), and could underlie the more recent (since 1993 and onwards) decrease in the  $\delta^{13}\text{C}$  of phytoplankton mirrored in our mussels. Similar multi-decadal decreasing trends for  $\delta^{13}\text{C}$  have been observed in bivalves (including *Mytilus*) from the English Channel and the Mediterranean Sea (Briant et al. 2018). A general decrease since the early 90s has also been demonstrated from various organisms and for different trophic levels in coastal and pelagic food webs of the in the North Sea and Baltic Sea, including Herring gull (Corman et al. 2018) and Atlantic salmon (Torniainen et al. 2014).

## 4.3. $\delta^{15}\text{N}$ pattern is region-specific for both taxa

The  $\delta^{15}\text{N}$  values were clearly region-specific for both taxa. The high and similar  $\delta^{15}\text{N}$  values of *Cladophora* and *Mytilus* from Askö archipelago were both linked to the high DIN concentration in this region. In this area, Savage and Elmgren (2004) described high  $\delta^{15}\text{N}$  values in *Fucus vesiculosus* close to a sewage outfall north of Askö archipelago but values were back to background level ( $\delta^{15}\text{N}$  of 4‰) towards the Askö island, 24 km away from the sewage outlet. The  $\delta^{15}\text{N}$  of *Cladophora* in our study remained high around Askö island (ca. 6.5‰). This could be explained by the higher nutrient uptake and growth rate of the seasonal filamentous algae with a high surface:volume ratio (Snoeijs-Leijonmalm 2017) compared to the slow growing perennial *Fucus* spp. (Wallentinus 1984), which makes *Cladophora* a more effective N-sink. The significant decrease in  $\delta^{15}\text{N}$  of the mussels in the Askö archipelago is statistically linked to the significant decrease in DIN in this area, reflecting the general decrease in land-based nutrient loadings over recent decades as a result of eutrophication mitigation (Savage et al. 2010; Elmgren et al. 2015), but also changes in internal denitrification potential from increased hypoxic waters since the 90s (Jäntti and Hietanen 2012). However, natural features such as coastal upwellings, which are frequent on the Swedish east coast of the Baltic Proper (Lehmann et al. 2012), also bear an enriched  $^{15}\text{N}$  signal that can contribute to high  $\delta^{15}\text{N}$  values in macrophytes (Marconi et al. 2011; Viana and Bode 2013). Bivalves including *Mytilus* can also capture the high  $\delta^{15}\text{N}$  signal from eutrophication (Fukumori et al. 2008; Carmichael et al. 2012; Thibault et al. 2020; Liénart et al. 2020) or from upwellings indirectly via plankton ingestion, as observed for invertebrates in other systems (e.g. Hill and McQuaid 2008). Similarly, Kiljunen et al. (2020) show increasing  $\delta^{15}\text{N}$  values from north to south of both pelagic and benthic baselines in the Baltic Sea, likely related to eutrophication patterns. In the Askö archipelago, both bulk  $\delta^{15}\text{N}$  and  $\delta^{15}\text{N}$  of phenylalanine ( $\delta^{15}\text{N}$ -Phe) for *Cladophora* were generally high and correlated, supporting the assimilation of  $^{15}\text{N}$  enriched nutrients in this area. For *Mytilus*, there was also a positive correlation between  $\delta^{15}\text{N}$ -bulk and  $\delta^{15}\text{N}$ -Phe, but  $\delta^{15}\text{N}$ -Phe values were much lower than for *Cladophora*, demonstrating differences in utilization of ultimate N sources, with negative values indicating diazotrophic N (Rolff 2000; Eglite et al. 2018). Alternatively, this may indicate different turnover time of N sources between these taxa. Indeed, low  $\delta^{15}\text{N}$  in *Mytilus* was explained by high amounts of  $\text{N}_2$ -fixing cyanobacteria and also linked to the mussel's condition index, indicating the role of physiology on bulk  $\delta^{15}\text{N}$  variability in the mussels, with lower  $\delta^{15}\text{N}$  indicative of better condition (Liénart et al. 2020). For *Mytilus*, slow N turnover (Smaal and Vonck 1997), and hence likely large  $^{15}\text{N}$  fractionation, may confound this signal in bulk  $\delta^{15}\text{N}$  values. Cyanobacterial N supports zooplankton and deposit-feeders during summer in the Baltic proper (Karlson et al. 2015), but there is currently no published study reporting active feeding of *Mytilus* on cyanobacteria. However, a recent experimental study suggests it is a relevant food source for the mussels during summer (Liénart et al. unpubl. data). At the open sea station of the Baltic Proper, where cyanobacterial N fixation is higher than in the coast (Olofsson et al. 2020). *Mytilus* bulk  $\delta^{15}\text{N}$  in this region was accordingly lower than in the Askö archipelago, better resembling the low  $\delta^{15}\text{N}$ -Phe in the mussels, and also lower in algae, possibly indirectly utilizing leaked N of cyanobacterial origin. Negative  $\delta^{15}\text{N}$ -Phe for particulate organic matter in surface water of Gotland has been confirmed previously (-1.7 to -6‰, Eglite et al. 2018). The large year-to-year variability in *Cladophora* bulk  $\delta^{15}\text{N}$ , and possibly in  $\delta^{15}\text{N}$ -Phe, can also occasionally reflect the influence of local upwellings at the southern tip of Gotland (Lehmann et al. 2012) bringing up more enriched  $^{15}\text{N}$  waters. In Höga Kusten, the low  $\delta^{15}\text{N}$  of *Cladophora* is likely related to the low  $\delta^{15}\text{N}$  signal of  $\text{NO}_3$  from pristine Nordic rivers ( $\delta^{15}\text{N}$ - $\text{NO}_3$  of  $0.6 \pm 1.1$ ‰,  $\delta^{15}\text{N}$ -PON of  $2.9 \pm 2.1$ ‰; Voss et al. 2005). However, increased cyanobacteria blooms in the coastal zone of the Bothnian Sea over the past decade (Andersson et al. 2015b; Olofsson et al. 2020) could additionally contribute to the low bulk  $\delta^{15}\text{N}$  and negative  $\delta^{15}\text{N}$ -Phe observed in both taxa here, especially in *Mytilus*.

#### 4.4. Different nutrient turnover rates in biota reflect system's nutrient dynamics

There were no significant differences in *Cladophora* and *Mytilus* N % or N:P across regions, with only P % significantly lower for both taxa in Gotland compared to the other regions (Table S5). However, the N:P of *Cladophora* was statistically linked to the water N:P ratio at a regional scale (simple linear model, Fig. S6), and this was supported at a local scale within the Askö archipelago (inner versus outer stations, Fig. S7). In our PLSR models, elemental composition for *Cladophora* was mainly linked to nutrient levels and, for P %, to summer maximum water temperature and phytoplankton bloom intensity, with a

larger bloom driving higher competition for nutrients and resulting in less light available. Nutrient concentrations in the water were generally higher for the Baltic Proper stations, and the DIN:DIP ratio was close to Redfield values in the Bothnian Sea (ca. 13) but N limited in the Baltic Proper (ca. 6–7, Fig. S5). The high nutrient absorption rates of *Cladophora* to sustain rapid growth during summer (Wallentinus 1984) can thus explain the correlation between the algal N:P ratio and nutrients levels in the water.

N:P ratio in *Mytilus* did not differ among regions, despite differences in nutrients and salinity, reflecting the relatively higher degree of homeostatic control consumers have over their elemental ratios. *Mytilus* has a low N turnover (Smaal and Vonck 1997), which likely explains the general absence of significant temporal trends and spatial pattern in elemental content of the mussels. A high N % in the mussels, used here as a proxy for protein content (Sterner and Elser 2002), was linked to higher condition index and lower temperature, with negative effects of higher temperatures on protein content expected. Similarly to the  $\delta^{15}\text{N}$  model, this highlights the importance of physiological processes for interpreting consumers' N elemental and isotope values. Nonetheless, *Mytilus* P %, used here as a proxy for growth (Elser et al. 2003), was significantly lower at the open sea station and was best explained by eutrophication and diet related predictors (dinoflagellates, diatoms). This highlights the importance of food quality for the growth of the mussels (e.g. Bracken 2017).

## 4.5. From nutrient to populations: understanding population level effects

Our data showed a rather similar biomass per  $\text{m}^2$  of *Cladophora* across the Baltic Sea, even though a strong year to year variability was observed within regions. There are no recent studies reporting *Cladophora* distribution, biomass or chemical composition in the Baltic Sea. Although *Cladophora* has been reported as increasing in the Baltic since the 1980s (Kraufvelin and Salovius 2004), our data did not show any significant temporal trends in *Cladophora* over the past two decades. That *Cladophora* thrive in shallow areas has been mainly discussed in relation to the eutrophication-induced decline of perennial brown macroalgae *Fucus* (Kautsky et al. 1986; Torn et al. 2006). The two macrophytes compete for space, light and nutrients (Kautsky et al. 1986), which could explain the rather high biomass of *Cladophora* in the Bothnian Sea where *Fucus* is absent due to low salinity levels. The biomass of *Cladophora* was linked to large-scale environmental conditions (i.e. Baltic Sea Index), and stable isotopes were also included as main predictors, with high  $\delta^{15}\text{N}$  potentially reflecting eutrophication. However, the biomass model had low explanatory and predictive capacities, and should be interpreted with caution. Adding predictors related to top-down control, such as grazing, and biomass of competitors for nutrients, like *Fucus*, would likely improve the model.

The biomass and abundance of *Mytilus* populations were low in the Bothnian Sea due to the low salinity of this area (as shown e.g. in the eastern Gulf of Finland, Westerborn et al. 2002). High mussel biomass was positively linked to higher nutrient concentration (DIN, DIP), with both decreasing as a result of eutrophication mitigation, although no corresponding decrease in total phytoplankton biovolume has been shown under this time period, with the opposite trend apparent at all regions (see Fig. S5 and Ek et al. 2021). However, compositional changes of phytoplankton have occurred (Fig. S5; Hjerne et al. 2019), which influence diet quality and hence the growth or survival of mussels (Liénart et al. 2020). For instance, the decrease in average mussel size ( $\text{Bm:Ab}_{\text{Mytilus}}$ ) in the Baltic Proper was linked to decrease in DIN but also to increase in  $\text{N}_2$ -fixing cyanobacteria blooms, a *Mytilus* food source whose quality is still debated. Finally, high biomass and large average mussel size were also linked to high  $\delta^{15}\text{N}$ , although  $\delta^{15}\text{N}$  was simultaneously linked to a lower condition index in individual mussels, which is contradictory. In general, the condition index was highest for the mussels at Höga Kusten. This is surprising considering the low salinity of the Baltic Proper, which is already at the *Mytilus* distribution area salinity limit of 4 (Snoeijs-Leijonmalm et al. 2017). One ecological explanation could be related to spawning, which is characterised by dramatic weight loss during early summer (up to 50%, Kautsky 1982). It is possible that spawning may not occur for mussels living at the salinity margin, hence resulting in a high condition index contrary to Askö archipelago mussels, which are likely now undergoing two spawning events per year (Westerborn pers. com.). Experimental studies testing the effects of the predictors discussed here on *Mytilus* individual growth and condition are hence needed to provide a mechanistic understanding for observed population biomass declines.

# Declarations

## Funding:

This project on retrospective chemical analyses of archived samples was funded by the Stockholm University Baltic Sea Centre and DEEP “seed” money to Agnes Karlson. The monitoring programs have over the years been financed by the Swedish Environmental Protection Agency and the Swedish Agency for Marine and Water Management. Part of the writing process was supported by a Walter and Andrée de Nottbeck post doctoral grant awarded to Camilla Liénart.

**Conflict of interest:** Not applicable.

**Availability of data and material:** The isotope metadata generated for this study are available open access at the Figshare data repository (doi: 10.6084/m9.figshare.14637804, only uploaded privately until acceptance of this manuscript).

**Code availability:** The code generated for this study are available on request to the corresponding author.

**Authors' contributions:** CL: Investigation, Formal Analyses, Writing-Original draft, AK: Conceptualization, Funding acquisition, Formal Analyses, Writing-Reviewing and Editing preparation, SQ: Investigation, Resources, Reviewing and Editing. AG: Resources, Writing- Reviewing and Editing.

**Ethics approval:** This study was carried out in accordance with the current laws in Sweden. There are no legal or ethical restrictions for invertebrates or macroalgae.

**Consent to participate:** All authors agreed on being co-authors of this manuscript.

**Consent for publication:** All authors agree on publishing the paper.

**Acknowledgments:** The monitoring program of phytobenthic communities was initiated by Hans Kautsky. Thanks to Ellen Schagerström for being part of recent years' field sampling. We thank Lydia Källberg Normark, Daniel Ahlström, Chiara D'agata, Adele Maciute, and Andrea De Cervo for assisting with sample preparation. We thank Hans-Harald Hinrichsen, who kindly provided the Baltic Sea Index (BSI) data, Siv Huseby for helping with interpreting environmental data from the Bothnian Sea and Jakob Walve, who provided unpublished environmental data for additional pelagic monitoring station at Askö. Thanks to Erik Smedberg for helping with the GIS map. We also thank François Méric and Fabian Bergland (MSc Students) for their preliminary analyses on the Askö local *Cladophora* data set. Sonja Repetti is thanked for proofreading this manuscript for English language. The authors declare there is no conflict of interest.

# References

1. Abrantes K, Sheaves M (2009) Food web structure in a near-pristine mangrove area of the Australian Wet Tropics. *Estuar Coast Shelf Sci* 82:597–607. <https://doi.org/10.1016/j.ecss.2009.02.021>
2. Anderson MJ, Gorley RN, Clarke KR (2008) PERMANOVA + for PRIMER. Guide to software and statistical methods. PRIMER-E: Plymouth, UK. 214 pp
3. Andersson A, Högländer H, Karlsson C, Huseby S (2015b) Key role of phosphorus and nitrogen in regulating cyanobacterial community composition in the northern Baltic Sea. *Estuar Coast Shelf Sci* 164:161–171. <https://doi.org/10.1016/j.ecss.2015.07.013>
4. Andersson A, Meier HEM, Ripszam M et al (2015a) Projected future climate change and Baltic Sea ecosystem management. *Ambio* 44:345–356. <https://doi.org/10.1007/s13280-015-0654-8>
5. Asmala E, Carstensen J, Conley DJ et al (2017) Efficiency of the coastal filter: Nitrogen and phosphorus removal in the Baltic Sea. *Limnol Oceanogr* 62:S222–S238. <https://doi.org/10.1002/lno.10644>

6. Asmala E, Carstensen J, Rake A (2019) Multiple anthropogenic drivers behind upward trends in organic carbon concentrations in boreal rivers. *Environ Res Lett* 14:. <https://doi.org/10.1088/1748-9326/ab4fa9>
7. Attard KM, Rodil IF, Berg P et al (2020) Metabolism of a subtidal rocky mussel reef in a high-temperate setting: pathways of organic C flow. *Mar Ecol Prog Ser* 645:41–45. <https://doi.org/10.3354/meps13372>
8. Bateman AS, Kelly SD (2007) Fertilizer nitrogen isotope signatures. *Isotopes Environ Health Stud* 43:237–247. <https://doi.org/10.1080/10256010701550732>
9. Bouwman AF, Bierkens MFP, Griffioen J et al (2013) Nutrient dynamics, transfer and retention along the aquatic continuum from land to ocean: towards integration of ecological and biogeochemical models. *Biogeosciences* 10:1–23. <https://doi.org/10.5194/bg-10-1-2013>
10. Bracken MES (2017) Stoichiometric mismatch between consumers and resources mediates the growth of rocky intertidal suspension feeders. *Front Microbiol* 8:1–10. <https://doi.org/10.3389/fmicb.2017.01297>
11. Briant N, Savoye N, Chouvelon T et al (2018) Carbon and nitrogen elemental and isotopic ratios of filter-feeding bivalves along the French coasts: An assessment of specific, geographic, seasonal and multi-decadal variations. *Sci Total Environ* 613–614:196–207. <https://doi.org/10.1016/j.scitotenv.2017.08.281>
12. Carmichael RH, Shriver AC, Valiela I (2012) Bivalve response to estuarine eutrophication: The balance between enhanced food supply and habitat alterations. *J Shellfish Res* 31:1–11. <https://doi.org/10.2983/035.031.0101>
13. Carstensen J, Conley DJ, Almroth-Rosell E et al (2020) Factors regulating the coastal nutrient filter in the Baltic Sea. *Ambio* 49:1194–1210. <https://doi.org/10.1007/s13280-019-01282-y>
14. Connolly RM, Gorman D, Hindell JS et al (2013) High congruence of isotope sewage signals in multiple marine taxa. *Mar Pollut Bull* 71:152–158. <https://doi.org/10.1016/j.marpolbul.2013.03.021>
15. Corman AM, Schwemmer P, Mercker M et al (2018) Decreasing  $\delta^{13}\text{C}$  and  $\delta^{15}\text{N}$  values in four coastal species at different trophic levels indicate a fundamental food-web shift in the southern North and Baltic Seas between 1988 and 2016. *Environ Monit Assess* 190:. <https://doi.org/10.1007/s10661-018-6827-8>
16. Doi H, Akamatsu F, Gonzalez AL (2017) Starvation effects on nitrogen and carbon stable isotopes of animals: An insight from meta-analysis of fasting experiments. *R Soc Open Sci* 4:. <https://doi.org/10.1098/rsos.170633>
17. Eglite E, Wodarg D, Dutz J et al (2018) Strategies of amino acid supply in mesozooplankton during cyanobacteria blooms: a stable nitrogen isotope approach. *Ecosphere* 9:e02135. <https://doi.org/10.1002/ecs2.2135>
18. Ek C, Faxneld S, Nyberg E et al (2021) The importance of adjusting contaminant concentrations using environmental data: A retrospective study of 25 years data in Baltic blue mussels. *Sci Total Environ* 762:. <https://doi.org/10.1016/j.scitotenv.2020.143913>
19. Elmgren R, Blenckner T, Andersson A (2015) Baltic Sea management: Successes and failures. *Ambio* 44:335–344. <https://doi.org/10.1007/s13280-015-0653-9>
20. Elser JJ, Acharya K, Kyle M et al (2003) Growth rate-stoichiometry couplings in diverse biota. *Ecol Lett* 6:936–943. <https://doi.org/10.1046/j.1461-0248.2003.00518.x>
21. Filgueira R, Comeau LA, Landry T et al (2013) Bivalve condition index as an indicator of aquaculture intensity: A meta-analysis. *Ecol Indic* 25:215–229. <https://doi.org/10.1016/j.ecolind.2012.10.001>
22. Franz M, Barboza FR, Hinrichsen HH et al (2019) Long-term records of hard-bottom communities in the southwestern Baltic Sea reveal the decline of a foundation species. *Estuar Coast Shelf Sci* 219:242–251. <https://doi.org/10.1016/j.ecss.2019.02.029>
23. Fry B, Sherr E (1984)  $^{13}\text{C}$  measurements as indicators of carbon flow in marine and freshwater ecosystems. *Contrib Mar Sci* 27:13–47
24. Fukumori K, Oi M, Doi H et al (2008) Bivalve tissue as a carbon and nitrogen isotope baseline indicator in coastal ecosystems. *Estuar Coast Shelf Sci* 79:45–50. <https://doi.org/10.1016/j.ecss.2008.03.004>

25. Gorokhova E (2018) Individual growth as a non-dietary determinant of the isotopic niche metrics. *Methods Ecol Evol* 9:269–277. <https://doi.org/10.1111/2041-210X.12887>
26. Gruber N, Keeling CD, Bacastow RB et al (1999) Spatiotemporal patterns of carbon-13 in the global surface ocean and the oceanic Suess effect. *Global Biogeochem Cycles* 13:307–335
27. HAVET (2015/2016) Havetrappporten/Sveriges vattenmiljö. Available from <http://havsmiljoinstitutet.se/publikationer/havet/havet2015-2016>. ISSN 1654–6741
28. Hemminga MA, Mateo MA (1996) Stable carbon isotopes in seagrasses: variability in ratios and use in ecological studies. *Mar Ecol Prog Ser* 140:285–298
29. Hill JM, McQuaid CD (2008)  $\delta^{13}\text{C}$  and  $\delta^{15}\text{N}$  biogeographic trends in rocky intertidal communities along the coast of South Africa: Evidence of strong environmental signatures. *Estuar Coast Shelf Sci* 80:261–268. <https://doi.org/10.1016/j.ecss.2008.08.005>
30. Hjerne O, Hajdu S, Larsson U et al (2019) Climate driven changes in timing, composition and magnitude of the Baltic Sea phytoplankton spring bloom. *Front Mar Sci* 6:482:1–15. <https://doi.org/10.3389/fmars.2019.00482>
31. Howell ET (2018) *Cladophora* (green algae) and dreissenid mussels over a nutrient loading gradient on the north shore of Lake Ontario. *J Great Lakes Res* 44:86–104. <https://doi.org/10.1016/j.jglr.2017.10.006>
32. Irisarri J, Fernández-Reiriz MJ, Labarta U (2015) Temporal and spatial variations in proximate composition and Condition Index of mussels *Mytilus galloprovincialis* cultured in suspension in a shellfish farm. *Aquaculture* 435:207–216. <https://doi.org/10.1016/j.aquaculture.2014.09.041>
33. Jäntti H, Hietanen S (2012) The effects of hypoxia on sediment nitrogen cycling in the Baltic Sea. *Ambio* 41:161–169. <https://doi.org/10.1007/s13280-011-0233-6>
34. Kahru M, Elmgren R (2014) Multidecadal time series of satellite-detected accumulations of cyanobacteria in the Baltic Sea. *Biogeosciences* 11:3619–3633. <https://doi.org/10.5194/bg-11-3619-2014>
35. Karlson AML, Duberg J, Motwani NH et al (2015) Nitrogen fixation by cyanobacteria stimulates production in Baltic food webs. *Ambio* 44:413–426. <https://doi.org/10.1007/s13280-015-0660-x>
36. Karlson AML, Faxneld S (2021) Polycyclic aromatic hydrocarbons and stable isotopes of carbon and nitrogen in Baltic Sea blue mussels: Time series data 1981–2016. *Data Br* 35:4–8. <https://doi.org/10.1016/j.dib.2021.106777>
37. Kautsky (1982) Quantitative studies on gonad cycle, fecundity, reproductive output and recruitment in a Baltic *Mytilus edulis* population. *Mar Biol* 68:143–160
38. Kautsky N, Evans S (1987) Role of biodeposition by *Mytilus edulis* in the circulation of matter and nutrients in a Baltic coastal ecosystem. *Mar Ecol Prog Ser* 38:201–212
39. Kautsky N, Kautsky H, Kautsky U, Waern M (1986) Decreased depth penetration of *Fucus vesiculosus* (L.) since the 1940's indicates eutrophication of the Baltic Sea. *Mar Ecol Prog Ser* 28:1–8
40. Kautsky N, Wallentinus I (1980) Nutrient release from a Baltic *Mytilus*-red algal community and its role in benthic and pelagic productivity. *Ophelia Suppl* 1:17–30
41. Kijewski TK, Zbawicka M, Väinölä R, Wenne R (2006) Introgression and mitochondrial DNA heteroplasmy in the Baltic populations of mussels *Mytilus trossulus* and *M. edulis*. *Mar Biol* 149:1371–1385. <https://doi.org/10.1007/s00227-006-0316-2>
42. Kiljunen M, Peltonen H, Lehtiniemi M et al (2020) Benthic-pelagic coupling and trophic relationships in northern Baltic Sea food webs. *Limnol Oceanogr* 65:1706–1722. <https://doi.org/10.1002/lno.11413>
43. Kraufvelin P, Salovius S (2004) Animal diversity in Baltic rocky shore macroalgae: can *Cladophora glomerata* compensate for lost *Fucus vesiculosus*? *Estuar Coast Shelf Sci* 61:369–378. <https://doi.org/10.1016/j.ecss.2004.06.006>
44. Larsson U, Hajdu S, Walve J, Elmgren R (2001) Baltic Sea nitrogen fixation estimated from the summer increase in upper mixed layer total nitrogen. *Limnol Oceanogr* 46:811–820

45. Ledesma M, Gorokhova E, Holmstrand H et al (2020) Nitrogen isotope composition of amino acids reveals trophic partitioning in two sympatric amphipods. *Ecol Evol* 10:10773–10784. <https://doi.org/10.1002/ece3.6734>
46. Lefebvre S, Marín Leal JC, Dubois S et al (2009) Seasonal dynamics of trophic relationships among co-occurring suspension-feeders in two shellfish culture dominated ecosystems. *Estuar Coast Shelf Sci* 82:415–425. <https://doi.org/10.1016/j.ecss.2009.02.002>
47. Lehmann A, Krauss W, Hinrichsen HH (2002) Effects of remote and local atmospheric forcing on circulation and upwelling in the Baltic Sea. *Tellus A Dyn Meteorol Oceanogr* 54:299–316. <https://doi.org/10.3402/tellusa.v54i3.12138>
48. Lehmann A, Myrberg K, Höflich K (2012) A statistical approach to coastal upwelling in the Baltic Sea based on the analysis of satellite data for 1990–2009. *Oceanologia* 54:369–393. <https://doi.org/10.5697/oc.54-3.369>
49. Liénart C, Garbaras A, Qvarfordt S et al (2020) Long-term changes in trophic ecology of blue mussels in a rapidly changing ecosystem. *Limnol Oceanogr Ino.*11633. <https://doi.org/10.1002/lno.11633>
50. Magni P, Rajagopal S, Como S et al (2013)  $\delta^{13}\text{C}$  and  $\delta^{15}\text{N}$  variations in organic matter pools, *Mytilus* spp. and *Macoma balthica* along the European Atlantic coast. *Mar Biol* 160:541–552. <https://doi.org/10.1007/s00227-012-2110-7>
51. Mäkinen A, Aulio K (1986) The use of *Cladophora glomerata* (Chlorophyta) to monitor levels of mineral nutrients in coastal waters. *Publications of the Water Research Institute* 68:160–163
52. Marconi M, Giordano M, Raven JA (2011) Impact of taxonomy, geography, and depth on  $\delta^{13}\text{C}$  and  $\delta^{15}\text{N}$  variation in a large collection of macroalgae. *J Phycol* 47:1023–1035. <https://doi.org/10.1111/j.1529-8817.2011.01045.x>
53. McClelland JW, Montoya JP (2002) Trophic relationships and the nitrogen isotopic composition of amino acids in plankton. *Ecology* 83:2173–2180. [https://doi.org/10.1890/0012-9658\(2002\)083\[2173:TRATNI\]2.0.CO;2](https://doi.org/10.1890/0012-9658(2002)083[2173:TRATNI]2.0.CO;2)
54. Middelburg JJ, Herman PMJ (2007) Organic matter processing in tidal estuaries. *Mar Chem* 106:127–147. <https://doi.org/10.1016/j.marchem.2006.02.007>
55. Oczkowski A, Taplin B, Pruell R et al (2018) Carbon stable isotope values in plankton and mussels reflect changes in carbonate chemistry associated with nutrient enhanced net production. *Front Mar Sci* 5:1–15. <https://doi.org/10.3389/fmars.2018.00043>
56. Olofsson M, Klawonn I, Karlson B (2020) Nitrogen fixation estimates for the Baltic Sea indicate high rates for the previously overlooked Bothnian Sea. *Ambio* 50:203–214. <https://doi.org/10.1007/s13280-020-01331-x>
57. Pernet F, Malet N, Pastoureaud A et al (2012) Marine diatoms sustain growth of bivalves in a Mediterranean lagoon. *J Sea Res* 68:20–32. <https://doi.org/10.1016/j.seares.2011.11.004>
58. Planas D, Maberly SC, Parker JE (1996) Phosphorus and nitrogen relationships of *Cladophora glomerata* in two lake basins of different trophic status. *Freshw Biol* 35:609–622. <https://doi.org/10.1111/j.1365-2427.1996.tb01772.x>
59. Post DM (2002) Using stable isotopes to estimate trophic position: models, methods, and assumptions. *Ecology* 83:703–718. [https://doi.org/10.1890/0012-9658\(2002\)083\[0703:USITET\]2.0.CO;2](https://doi.org/10.1890/0012-9658(2002)083[0703:USITET]2.0.CO;2)
60. Quay P, Sonnerup R, Stutsman J et al (2007) Anthropogenic  $\text{CO}_2$  accumulation rates in the North Atlantic Ocean from changes in the  $^{13}\text{C}/^{12}\text{C}$  of dissolved inorganic carbon. *Global Biogeochem Cycles* 21:1–15. <https://doi.org/10.1029/2006GB002761>
61. R Core Team (2020) R: A language and environment for statistical computing. R Foundation for Statistical Computing, Vienna, Austria. <https://www.R-project.org/>, version 4.0.3 (2020-10-10)
62. Råberg S (2004) Competition from filamentous algae on *Fucus vesiculosus* - negative effects and the implications on biodiversity of associated flora and fauna. *Plant Ecology*, vol. 4. Licenciate Thesis. Department of Botany, Stockholm University, pp. 1–26
63. Räisänen J (2017) Future climate change in the Baltic Sea region and environmental impacts. In: H V, Storch (eds) *Oxford Research Encyclopedias : Climate Science*. Oxford University Press, Oxford. <https://doi.org/10.1093/acrefore/9780190228620.013.634>

64. Rinne H, Salovius-laurén S (2020) The status of brown macroalgae *Fucus* spp. and its relation to environmental variation in the Finnish marine area, northern Baltic Sea. *Ambio* 49:118–129. <https://doi.org/10.1007/s13280-019-01175-0>
65. Rolff C (2000) Seasonal variation in delta C-13 and delta N-15 of size-fractionated plankton at a coastal station in the northern Baltic proper. *Mar Ecol Ser* 203:47–65. <https://doi.org/10.3354/meps203047>
66. Rolff C, Elfving T (2015) Increasing nitrogen limitation in the Bothnian Sea, potentially caused by inflow of phosphate-rich water from the Baltic Proper. *Ambio* 44:601–611. <https://doi.org/10.1007/s13280-015-0675-3>
67. Rolff C, Elmgren R (2000) Use of riverine organic matter in plankton food webs of the Baltic Sea. *Mar Ecol Prog Ser* 197:81–101
68. Savage C, Elmgren R (2004) N values trace decrease in sewage influence. *Ecol Appl* 14:517–526. <https://doi.org/10.1890/02-5396>
69. Savage C, Leavitt PR, Elmgren R (2010) Effects of land use, urbanization, and climate variability on coastal eutrophication in the Baltic Sea. *Limnol Oceanogr* 55:1033–1046. <https://doi.org/10.4319/lo.2010.55.3.1033>
70. Savchuk OP (2018) Large-Scale Nutrient Dynamics in the Baltic Sea, 1970–2016. *Front Mar Sci* 5:1–20. <https://doi.org/10.3389/fmars.2018.00095>
71. Schloesser RW, Rooker JR, Louchuam P et al (2009) Interdecadal variation in seawater  $\delta^{13}\text{C}$  and  $\delta^{18}\text{O}$  recorded in fish otoliths. *Limnol Oceanogr* 54:1665–1668. <https://doi.org/10.4319/lo.2009.54.5.1665>
72. Smaal AC, Vonck APMA (1997) Seasonal variation in C, N and P budgets and tissue composition of the mussel *Mytilus edulis*. *Mar Ecol Prog Ser* 153:167–179. <https://doi.org/10.3354/meps153167>
73. Snoeijs-Leijonmalm P, Schubert H, Radziejewska T (2017) Biological oceanography of the Baltic Sea. Springer, Netherlands, p 683. doi:10.1007/978-94-007-0668-2
74. Stepien CC (2015) Impacts of geography, taxonomy and functional group on inorganic carbon use patterns in marine macrophytes. *J Ecol* 103:1372–1383. <https://doi.org/10.1111/1365-2745.12451>
75. Sterner RW, Elser JJ (2002) Ecological stoichiometry, the biology of elements from molecules to the biosphere. Princeton Univ. Press, Princeton
76. Stuckas H, Stoof K, Quesada H, Tiedemann R (2009) Evolutionary implications of discordant clines across the Baltic *Mytilus* hybrid zone (*Mytilus edulis* and *Mytilus trossulus*). *Heredity* 103:146–156. <https://doi.org/10.1038/hdy.2009.37>
77. Takolander A, Cabeza M, Leskinen E (2017) Climate change can cause complex responses in Baltic Sea macroalgae: A systematic review. *J Sea Res* 123:16–29. <https://doi.org/10.1016/j.seares.2017.03.007>
78. Tedengren M, Kautsky N (1987) Comparative stress response to diesel oil and salinity changes of the blue mussel, *Mytilus edulis* from the Baltic and North Seas. *Ophelia* 28:1–9. <https://doi.org/10.1080/00785326.1987.10430800>
79. Thibault M, Duprey N, Gillikin DP et al (2020) Bivalve  $\delta^{15}\text{N}$  isoscapes provide a baseline for urban nitrogen footprint at the edge of a World Heritage coral reef. *Mar Pollut Bull* 152:110870. <https://doi.org/10.1016/j.marpolbul.2019.110870>
80. Thybo-Christesen M, Rasmussen MB, Blackburn TH (1993) Nutrient fluxes and growth of *Cladophora sericea* in a shallow Danish bay. *Mar Ecol Prog Ser* 100:273–281
81. Torn K, Krause-Jensen D, Martin G (2006) Present and past depth distribution of bladderwrack (*Fucus vesiculosus*) in the Baltic Sea. *Aquat Bot* 84:53–62. <https://doi.org/10.1016/j.aquabot.2005.07.011>
82. Torniaainen J, Vuorinen PJ, Jones RI et al (2014) Migratory connectivity of two Baltic Sea salmon populations: retrospective analysis using stable isotopes of scales. *ICES J Mar Sci* 71:336–344. <https://doi.org/10.1093/icesjms/fst153>
83. Vahtera E, Conley DJ, Gustafsson BG et al (2007) Internal ecosystem feedbacks enhance nitrogen-fixing cyanobacteria blooms and complicate management in the Baltic Sea. *Ambio* 36:186–194
84. Vander Zanden MJ, Rasmussen JB (1999) Variation in  $\delta^{13}\text{C}$  and  $\delta^{15}\text{N}$  trophic fractionation: Implications for aquatic food web studies. *Limnol Oceanogr* 46:2061–2066. <https://doi.org/10.4319/lo.2001.46.8.2061>

85. Viana IG, Bode A (2013) Stable nitrogen isotopes in coastal macroalgae: Geographic and anthropogenic variability. *Sci Total Environ* 443:887–895. <https://doi.org/10.1016/j.scitotenv.2012.11.065>
86. Voss M, Emeis KC, Hille S et al (2005) Nitrogen cycle of the Baltic Sea from an isotopic perspective. *Global Biogeochem Cycles* 19:1–15. <https://doi.org/10.1029/2004GB002338>
87. Voss M, Larsen B, Leivuori M, Vallius H (2000) Stable isotope signals of eutrophication in Baltic Sea sediments. *J Mar Syst* 25:287–298. [https://doi.org/10.1016/S0924-7963\(00\)00022-1](https://doi.org/10.1016/S0924-7963(00)00022-1)
88. Vuorinen I, Hänninen J, Rajasilta M et al (2015) Scenario simulations of future salinity and ecological consequences in the Baltic Sea and adjacent North Sea areas-implications for environmental monitoring. *Ecol Indic* 50:196–205. <https://doi.org/10.1016/j.ecolind.2014.10.019>
89. Wallentinus I (1984) Comparison of nutrient uptake rates for Baltic macroalgae with different thallus morphologies. *Mar Biol* 80:215–225
90. Westerbom M, Kilpi M, Mustonen O (2002) Blue mussels, *Mytilus edulis*, at the edge of the range: population structure, growth and biomass along a salinity gradient in the north-eastern Baltic Sea. *Mar Biol* 140:991–999. <https://doi.org/10.1007/s00227-001-0765-6>
91. Westerbom M, Mustonen O, Jaatinen K et al (2019) Population Dynamics at the Range Margin: Implications of Climate Change on Sublittoral Blue Mussels (*Mytilus trossulus*). *Front Mar Sci* 6:1–10. <https://doi.org/10.3389/fmars.2019.00292>
92. Westerbom M, Mustonen O, Kilpi M (2008) Distribution of a marginal population of *Mytilus edulis*: responses to biotic and abiotic processes at different spatial scales. *Mar Biol* 135:1153–1164. <https://doi.org/10.1007/s00227-007-0886-7>
93. Wiencke C, Fischer G (1990) Growth and stable carbon isotope composition of cold-water macroalgae in relation to light and temperature. *Mar Ecol Prog Ser* 65:283–292
94. Wikner J, Andersson A (2012) Increased freshwater discharge shifts the trophic balance in the coastal zone of the northern Baltic Sea. *Glob Chang Biol* 18:2509–2519. <https://doi.org/10.1111/j.1365-2486.2012.02718.x>
95. Willis TV, Wilson KA, Johnson BJ (2017) Diets and stable isotope derived food web structure of fishes from the inshore Gulf of Maine. *Estuaries Coasts* 40:889–904. <https://doi.org/10.1007/s12237-016-0187-9>
96. Wold S, Sjöström M, Eriksson L (2001) PLS-regression: a basic tool of chemometrics. *Chemom Intell Lab Syst* 58:109–130. [https://doi.org/10.1016/S0169-7439\(01\)00155-1](https://doi.org/10.1016/S0169-7439(01)00155-1)
97. Zulkifly SB, Graham JM, Young EB et al (2013) The genus *Cladophora* Kützinger (Ulvophyceae) as a globally distributed ecological engineer. *Phycol Soc Am* 49:1–17. <https://doi.org/10.1111/jpy.12025>

## Figures

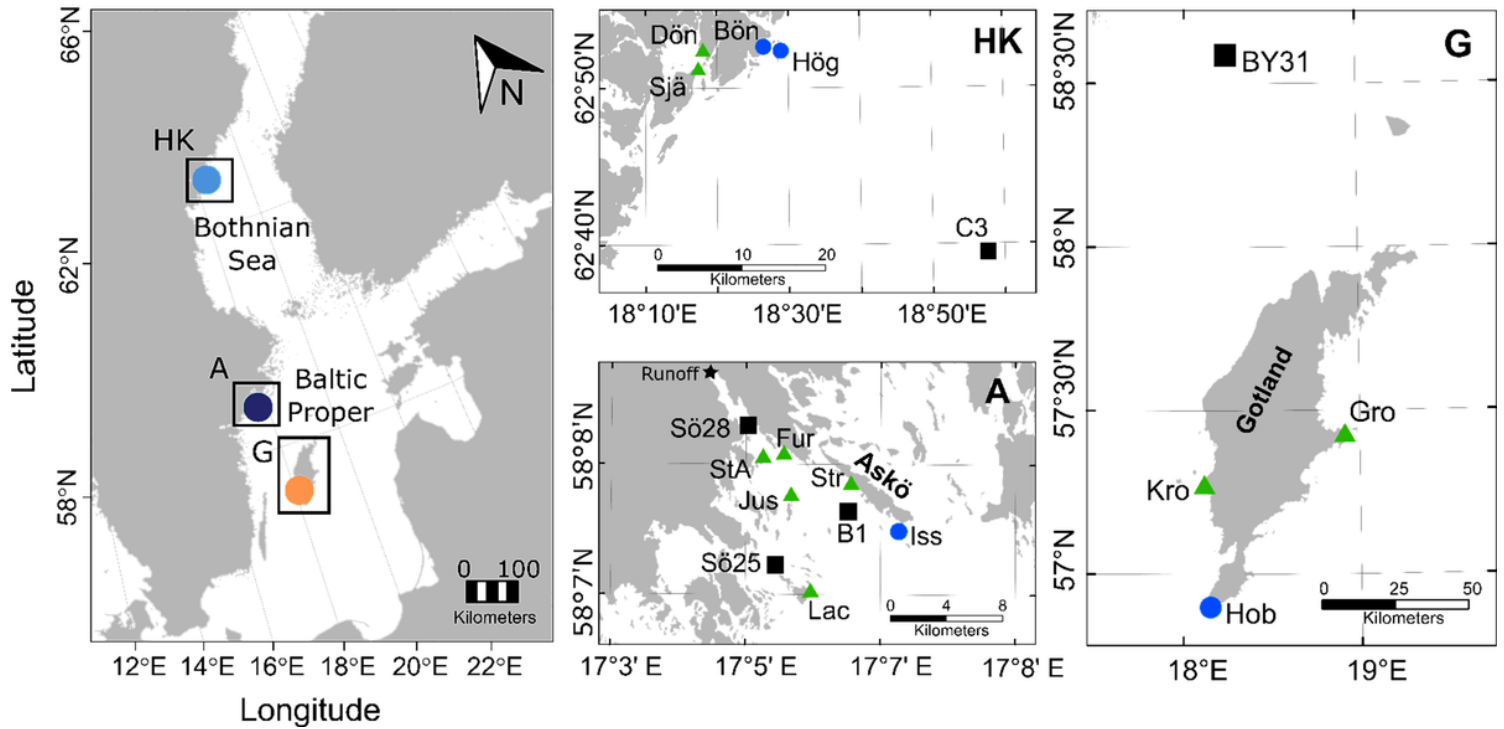


**Figure 1**

Study regions of the Bothnian Sea (HK: Höga Kusten) and the Baltic Proper (A: Archipelago close to Askö field station, and G: Gotland island). Stations within each region are shown in the three right panels: green triangles are *Cladophora* sampling stations only, blue circles are *Mytilus* and *Cladophora* sampling stations, black squares are pelagic environmental monitoring stations. Note: The designations employed and the presentation of the material on this map do not imply the expression of any opinion whatsoever on the part of Research Square concerning the legal status of any country, territory, city or area or of its authorities, or concerning the delimitation of its frontiers or boundaries. This map has been provided by the authors.

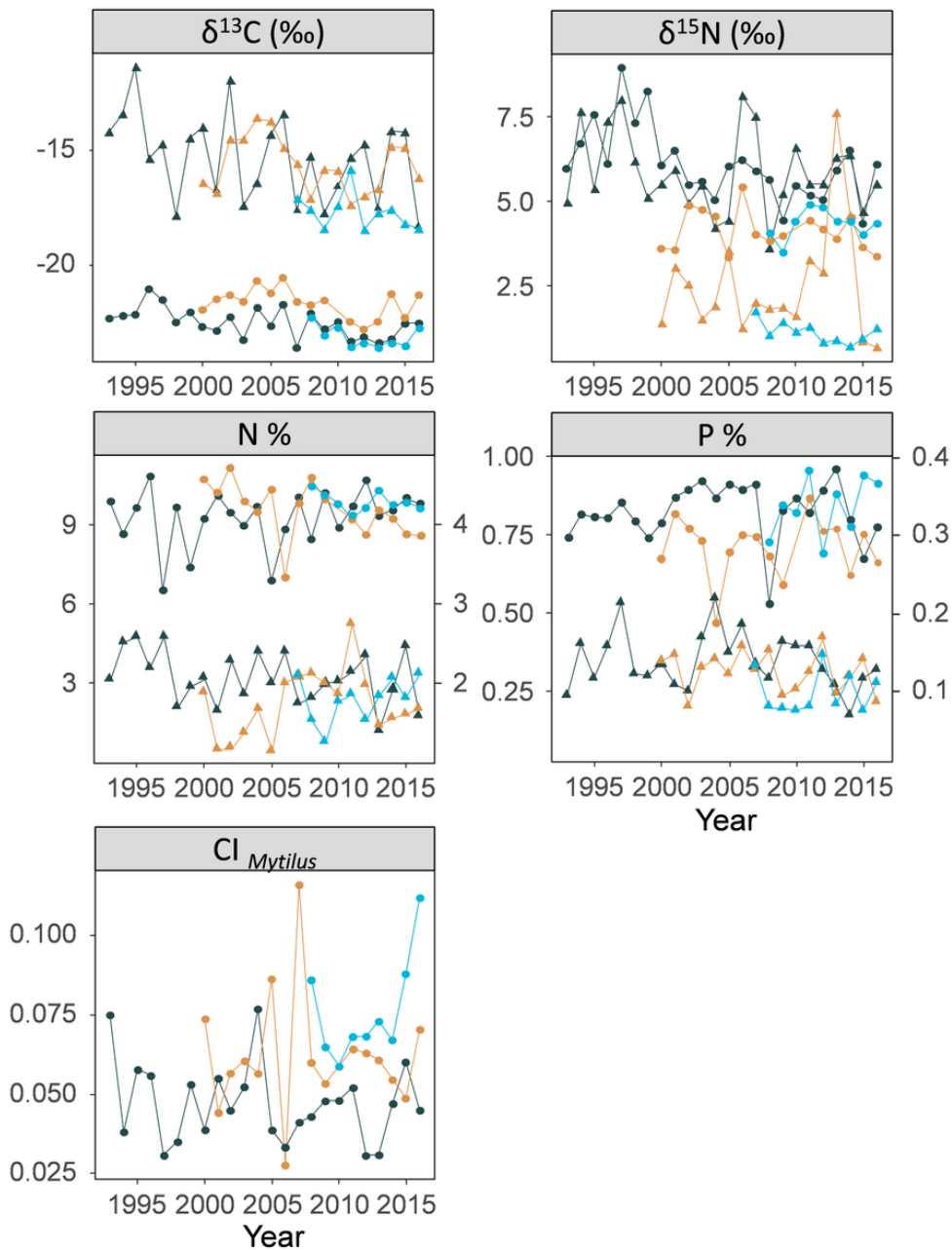


**Figure 2**

Temporal trends in elemental and isotope composition of *Cladophora* (triangles) and *Mytilus* (circles) from the 3 regions (Archipelago: black, Gotland: orange, Höga Kusten: blue). Variables with dual axis (N and P %): the axis on the left is for *Mytilus* and the axis on the right is for *Cladophora*. For a multivariate summary of region-specific pattern see Fig S2.

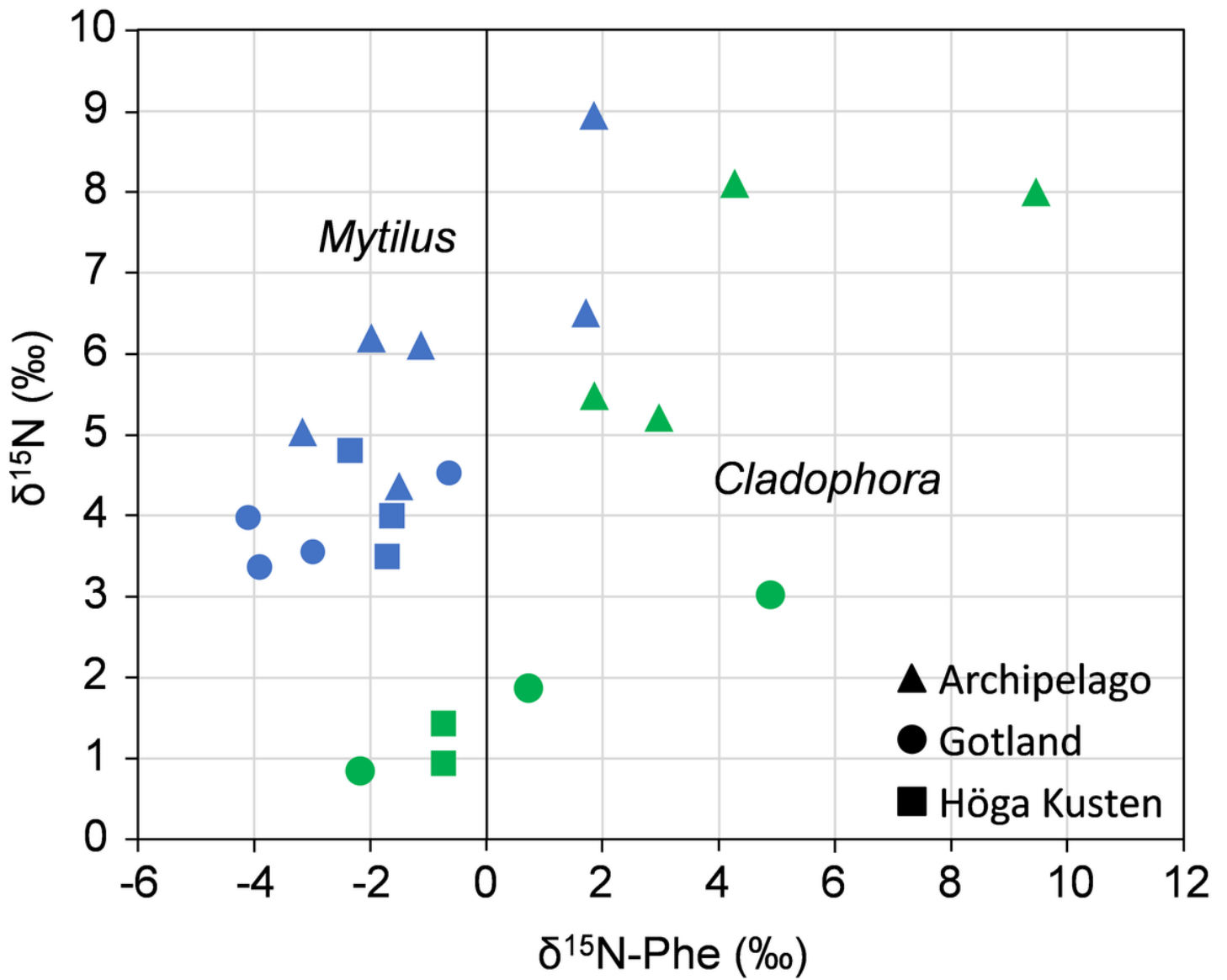
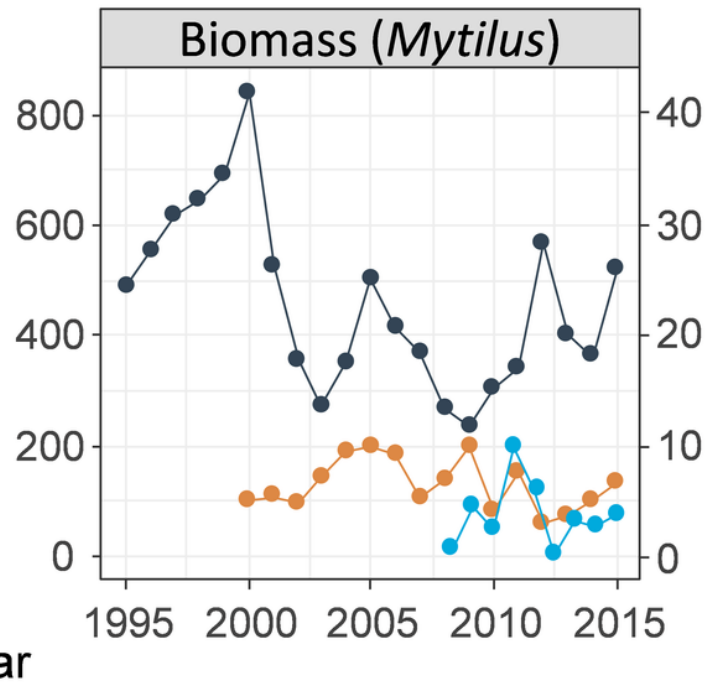
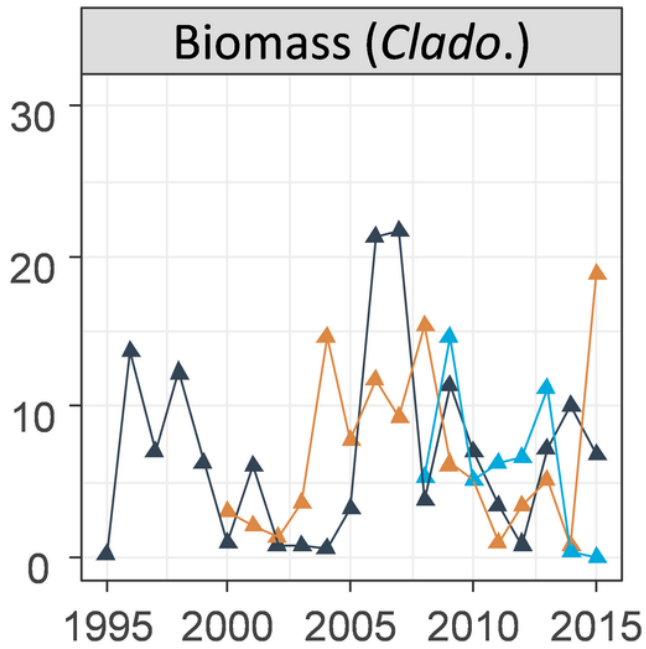


Figure 3

Nitrogen isotope ratio of the source amino-acid phenylalanine ( $\delta^{15}\text{N-Phe}$ ) for *Mytilus* (blue) and *Cladophora* (green) of the 3 regions.



**Figure 4**

Temporal trends in Cladophora (triangles) and Mytilus (circles) population biomass (g dry weight per m<sup>2</sup>) from the 3 regions (Archipelago: black, Gotland: orange, Höga Kusten: blue). For Mytilus biomass, the left axis indicates Askö archipelago and Gotland and the axis on the right indicates Höga Kusten.

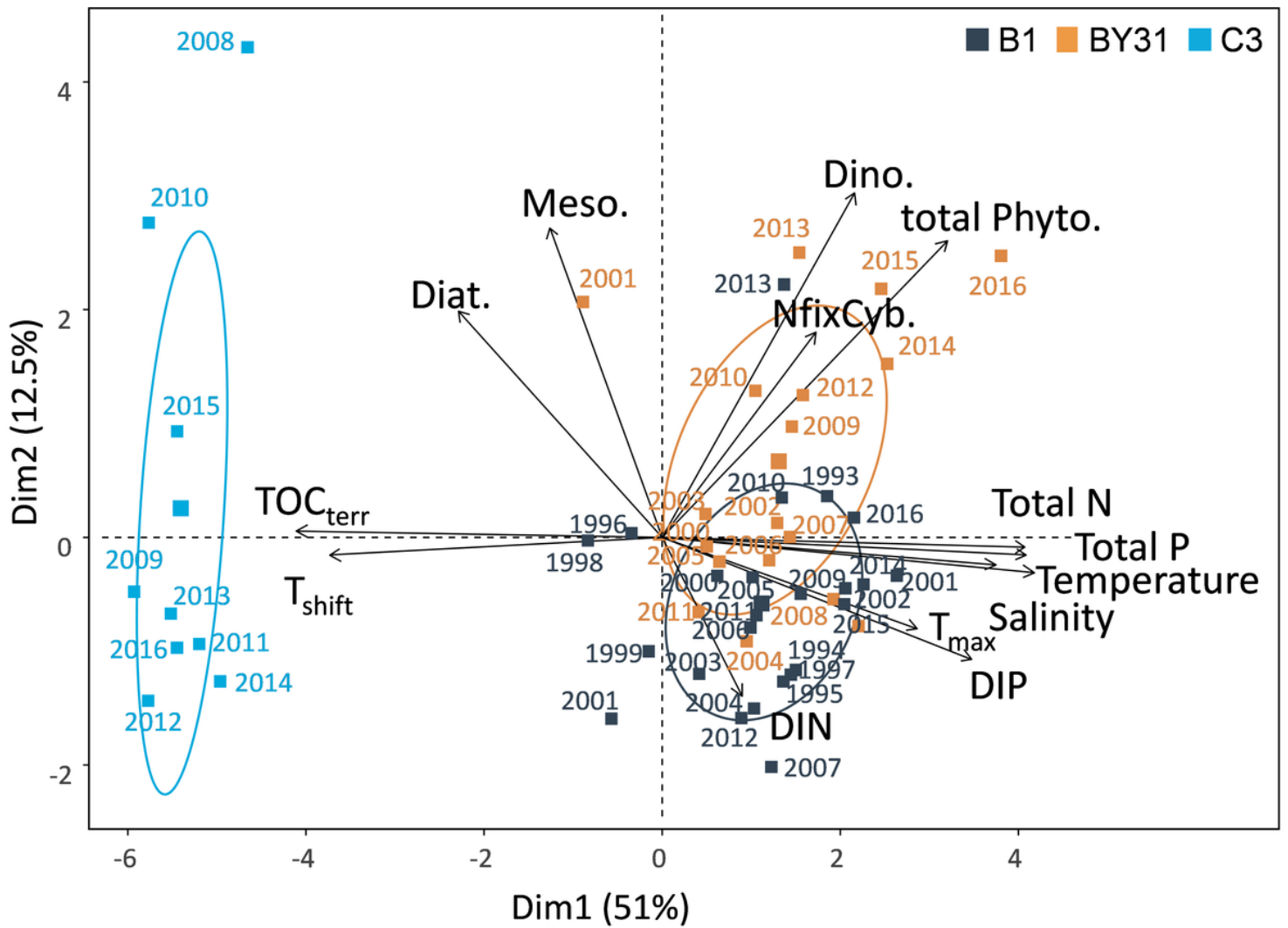


**Figure 5**

Principal component analysis (PCA) of environmental variables for B1 (black), BY31 (orange) and C3 (blue). Scaled data. Ellipses represent 50% of the data. See Fig. S5 for the raw dataset over time. T<sub>max</sub>: water maximum temperature in summer, DIN or DIP: Dissolved Inorganic Nitrogen / Phosphorus, TOC<sub>terr</sub>: total organic carbon from land, T<sub>shift</sub>: water temperature shift, Diat.: diatom, Dino.: dinoflagellates, Meso.: *Mesodinium rubrum*, NfixCyb.: N<sub>2</sub>-fixing cyanobacteria.

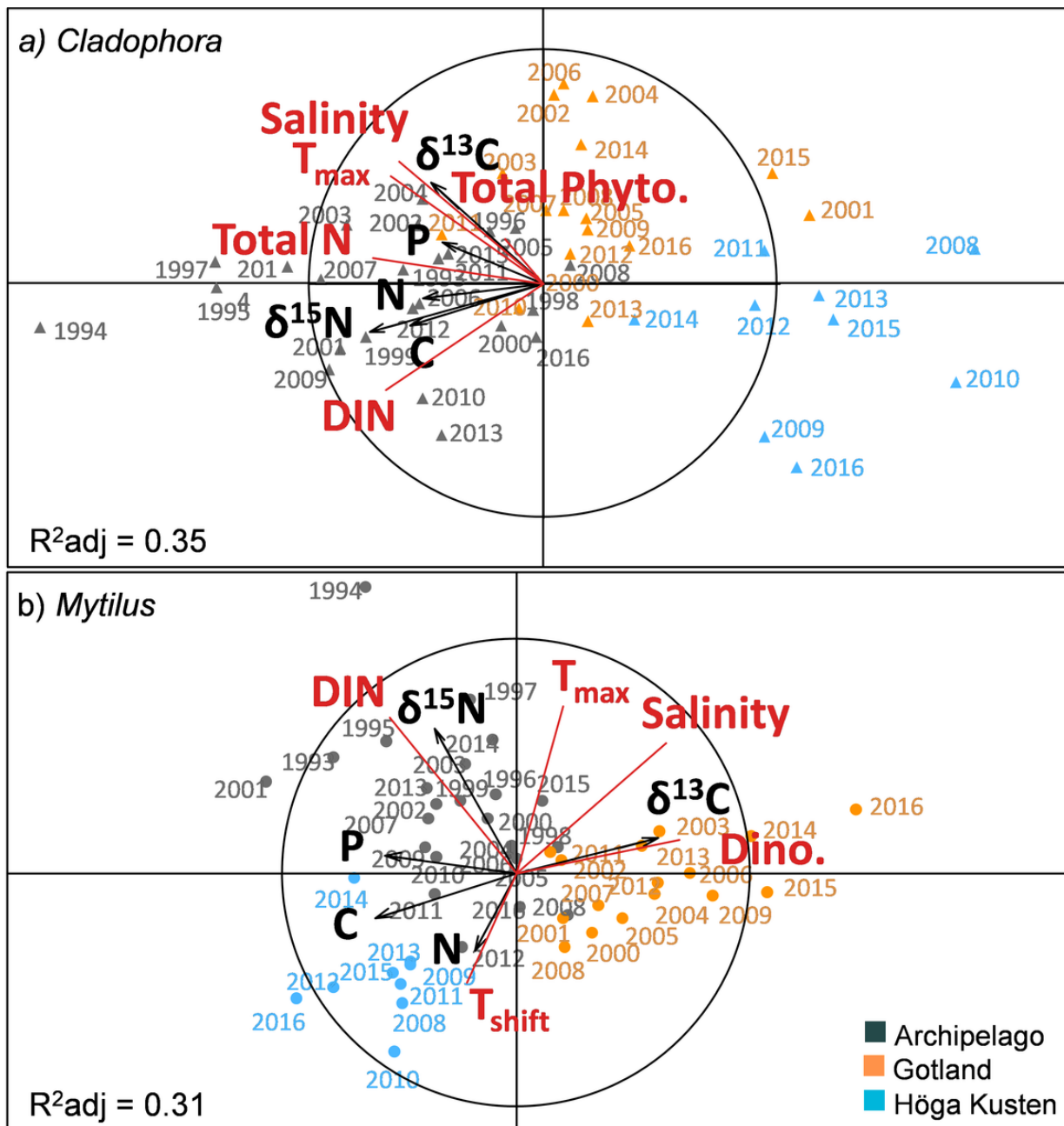


Figure 6

Principal component analysis (PCA) of environmental variables for B1 (black), BY31 (orange) and C3 (blue). Scaled data. Ellipses represent 50% of the data. See Fig. S5 for the raw dataset over time. T<sub>max</sub>: water maximum temperature in summer, DIN or DIP: Dissolved Inorganic Nitrogen / Phosphorus, TOC<sub>terr</sub>: total organic carbon from land, T<sub>shift</sub>: water temperature shift, Diat.: diatom, Dino.: dinoflagellates, Meso.: *Mesodinium rubrum*, NfixCyb.: N<sub>2</sub>-fixing cyanobacteria.

## Supplementary Files

This is a list of supplementary files associated with this preprint. Click to download.

- [SupplementalmaterialLSVF.docx](#)